The AHR target gene Scinderin activates the WNT pathway by facilitating the nuclear translocation of β-catenin

Lizbeth Perez-Castro[1,*], Niranjan Venkateswaran[1,*], Roy Garcia[1], Yi-Heng Hao[1], M. Carmen Lafita-Navarro[1], Jiwoong Kim[2], Dagan Segal[1,6], Etai Saponzik[6], Bo-Jui Chang[6], Reto Fiolka[6], Gaudenz Danuser[1,6], Lin Xu[2,3,4], Thomas Brabletz[7], and Maralice Conacci-Sorrell[1,3,5,‡]

[1]Department of Cell Biology, UT Southwestern Medical Center, Dallas, TX 75390, USA

[2]Quantitative Biomedical Research Center, Department of Population & Data Sciences, University of Texas Southwestern Medical Center, Dallas, TX 75390, USA

[3]Harold C. Simmons Comprehensive Cancer Center, UT Southwestern Medical Center, Dallas, TX 75390, USA

[4]Department of Pediatrics, Division of Hematology/Oncology, UT Southwestern Medical Center, Dallas, TX 75390, USA

[5]Hamon Center for Regenerative Science and Medicine, University of Texas Southwestern Medical Center, Dallas, TX 75390, USA

[6]Lyda Hill Department of Bioinformatics, UT Southwestern Medical Center, Dallas, TX 75390, USA

[7]Nikolaus-Fiebiger Center for Molecular Medicine, University Erlangen-Nurnberg, Erlangen 91054, Germany

[*]Equal contribution

[‡]Author for correspondence: Maralice.ConacciSorrell@UTSouthwestern.edu

Key words: TCDD, kynurenine, FICZ, aryl hydrocarbon receptor, AHR, colon cancer

ABSTRACT

The ligand-activated transcription factor Aryl Hydrocarbon Receptor (AHR) regulates cellular detoxification, proliferation, and immune evasion in a range of cell types and tissues, including cancer cells. In this study, we used RNA-seq to identify the signature of AHR target genes regulated by the pollutant 2,3,7,8-tetrachlorodibenzodioxin (TCDD) and the endogenous ligand kynurenine (Kyn), a tryptophan-derived metabolite. This approach identified a signature of six genes (*CYP1A1*, *ALDH1A3*, *ABCG2*, *ADGFR1*, and SCIN) as commonly activated by endogenous or exogenous ligands of AHR in multiple colon cancer cell lines. Among these, the actin-severing protein Scinderin (SCIN) was necessary for cell proliferation; SCIN downregulation limited cell proliferation and its expression increased it. SCIN expression is elevated in a subset of colon cancer patient samples, which also contain elevated β-catenin levels. Remarkably, SCIN expression promotes nuclear translocation of β-catenin and activates the WNT pathway. Our study identified a new mechanism for adhesion-mediated signaling in which SCIN, likely via its ability to alter the actin cytoskeleton, facilitates the nuclear translocation of β-catenin.

INTRODUCTION

Aryl hydrocarbon receptor (AHR) is one of the most well-studied sensors for environmental toxins, including polyaromatic hydrocarbons and other xenobiotics such as TCDD (Denison and Nagy, 2003). These small molecules function as ligands for AHR driving its nuclear translocation and the transcriptional activation of AHR target genes. In addition, several endogenous small molecules, such as the tryptophan-derived metabolites Kyn and 6-formylindolo[3,2-b]carbazole (FICZ), and the plant-derived compound quercetin also function as ligands for AHR (Denison and Nagy, 2003; Murray et al., 2014; Van der Heiden et al., 2009).

In absence of ligands, AHR is maintained in the cytoplasm by a complex containing heat shock protein 90 (HSP90) and X-associated protein 2 (XAP2) (Feng et al., 2013; Fukunaga et al., 1995). Binding of AHR to its ligands causes a conformational change that leads to the exposure

of the nuclear localization signal of AHR (Ikuta et al., 2000). This results in the translocation of AHR to the nucleus where it binds to Aryl Hydrocarbon Receptor Nuclear Translocator (ARNT) to form a transcriptionally active complex. This complex then binds to Xenobiotic Response Elements (XRE) present in the promoters of its target genes, including those involved in detoxification pathways, to activate their transcription (Matthews et al., 2005; Yao and Denison, 1992).

In addition to regulating xenobiotic response, AHR is also implicated in coordinating several critical pathways, including adaptive immunity, gut homeostasis, and secretion of cytokines (Rothhammer and Quintana, 2019). AHR expression is elevated in tumor tissues of multiple origins including lung, breast, and colon (Koliopanos et al., 2002; Kubli et al., 2019; Lafita-Navarro et al., 2018; Opitz et al., 2011; Tsay et al., 2013; Venkateswaran et al., 2019; Xie et al., 2012). Nevertheless, the role of AHR in colon cancer is complex. Studies show that embryonic deletion of AHR from colonic cells leads to increased proliferation and exacerbates the growth of colon cancer tumor models (Han et al., 2021; Murray et al., 2014; Narasimhan et al., 2018). In addition, ablation of AHR was shown to accelerate intestinal tumor formation by stabilizing β-catenin through mechanisms unrelated to the transcriptional activity of AHR (Ikuta et al., 2013; Kawajiri et al., 2009).

The role of AHR in cancer is likely influenced by its binding to specific ligands and the landscape of oncogenes/tumor suppressors of each cell type. Our lab previously found that AHR is transcriptionally induced by the universal oncogene MYC in colon cancer cells and that AHR supports MYC-induced proliferation (Lafita-Navarro et al., 2018) by activating the expression of genes necessary for biomass production (Lafita-Navarro et al., 2018; Lafita-Navarro et al., 2020a; Lafita-Navarro et al., 2020b). MYC also promotes the uptake of tryptophan and its conversion into Kyn in colon cancer cells (Venkateswaran and Conacci-Sorrell, 2020; Venkateswaran et al., 2019b), thus leading to nuclear translocation of AHR in these cells (Venkateswaran et al., 2019b). AHR activation by TCDD was found to drive colon cancer cell survival and migration (Xie et al., 2012) and that expression of a constitutively active AHR causes stomach cancer (Andersson et al., 2002).Additionally, the TDO2-AHR pathway is necessary for colon cancers to metastasize to the liver (Miyazaki et al., 2022) and AHR promote chemoresistance in cancers (Li et al., 2021; Stanford et al., 2016; Wu et al., 2018). Moreover,

Inhibition of the Kyn-AHR axis can improve anti-cancer immunity preventing colitis-associated cancer (Campesato et al., 2020; Zhang et al., 2021)

The diversity of the cellular functions exhibited by AHR highlights the need to identify tumor-specific genes directly regulated by AHR and its ligands. To investigate the effects of exogenous and endogenous ligands of AHR on the transcriptional profile of colon cancer cells, we performed RNA-seq comparing colon cancer cells exposed to TCDD, Kyn, and the AHR inhibitor CH223191. This approach identified a 6-gene signature containing Cytochrome P450 Family 1 Subfamily A Member 1 *(CYP1A1)*, Aldehyde Dehydrogenase 1 Family Member A3 *(ALDH1A3)*, ATP Binding Cassette Subfamily G Member 2 *(ABCG2)*, Adhesion G Protein-Coupled Receptor F1 *(ADGFR1)*, and the actin-severing protein Scinderin (*SCIN*) as activated by both Kyn and TCDD in colon cancer cells. TCDD activated additional genes, including genes previously shown to function as oncogenes. Among genes identified in our screen, *SCIN* was found to be necessary for cell growth due to its newly discovered ability to activate the WNT pathway.

RESULTS

Transcriptional signatures regulated by TCDD and Kyn in colon cancer cells

Elevated levels of AHR were detected in many tumors deposited in the TCGA database, including colon cancer (Fig. S1A), and its expression in the colon coincides with increased expression of the oncogene MYC (Fig. S1B). These data support data from the previously published studies that documented elevated levels of AHR in colon cancer cell lines and patient samples (Lafita-Navarro et al., 2018; Venkateswaran and Conacci-Sorrell, 2020; Venkateswaran et al., 2019b). Therefore, we selected colon cancer cells as a model system to study AHR transcriptional activity upon ligand stimulation. To pick a colon cancer cell line for transcriptional profiling, we performed RT-qPCR for *AHR* in multiple colon cancer cell lines including DLD1, RKO, HCT115, HCT116, and HT29. DLD1 cells expressed the highest levels of *AHR* among the analyzed cell lines (Fig. 1A). Knocking down AHR through siRNA transfection in colon cancer cells led to a reduction in viability of DLD1 and HT29 cells (Fig 1B, 1C, Fig S1C) but not HCT116 cells (Fig. 1D). DLD1 cells stably expressing an AHR shRNA displayed a similar decrease in proliferation as with transient knockdown (Fig S1D). While there was nuclear AHR, the majority of AHR protein was localized in the cytoplasm of DLD1 cells as

demonstrated by Western blotting the nuclear and cytoplasmic fractions (Fig. S1E). Because AHR mRNA and cytoplasmic protein levels were elevated in DLD1 cells, we chose DLD1 to identify transcriptional targets of AHR regulated by ligand stimulation.

To compare the signature of genes induced by endogenous and exogenous AHR ligands, we performed RNA-seq of DLD1 cells incubated with vehicle (DMSO), TCDD, or Kyn for 8 h (Fig. 1E-F, 1H-I). The 8-h incubation time was chosen to increase the probabilities of identifying early transcriptional responses to TCDD and Kyn. Using a cutoff of $\log_2$FC $\leq$0.585 and adjusted P value $\leq$0.05, we identified 40 genes regulated by TCDD (39 up regulated and 1 downregulated) (Fig. 1E) and 6 genes upregulated by Kyn (Fig. 1F). The higher number of genes activated by TCDD may be explained by a previous finding that demonstrated TCDD binds to AHR with higher affinity than Kyn (Denison et al., 2002). It is also possible that TCDD may have the ability to maintain a sustained activation of AHR, thus leading to the activation of a larger number of genes. Despite the different number of target genes activated by TCDD and Kyn, gene ontology analyses found that the most significant pathway regulated by both ligands was xenobiotic response (Fig. 1H-J). Thus, these data suggest that both endogenous and exogenous ligands support the ability of AHR to activate genes necessary for xenobiotic response.

In addition to activating Kyn-regulated genes (Fig. 1F, 1I), TCDD also activated genes involved in multiple cellular processes (Fig. 1L) including cell growth such as: Fibroblast Growth Factor Binding Protein 1 (*FGFBP1*), Prospero Homeobox 1 (*PROX1*), Proto-Oncogene Serine/Threonine-Protein Kinase Pim-1 (*PIM1*), and Alkaline Phosphatase Placental type (*ALPP*) (Fig. S2A). FGFBP1 is a fibroblast-secreted growth factor previously shown to play key roles in pancreatic and colorectal carcinogenesis (Tassi et al., 2006). PROX1 is a transcription factor essential during development. Increased levels of PROX1 have been observed in a variety of cancers including colon, breast and liver (Elsir et al., 2012; Petrova et al., 2008). PIM1 is a Ser/Thr kinase and an oncogene identified in T-cell lymphomas and pancreatic cancer shown to increase cell cycle regulation and cellular proliferation (Tursynbay et al., 2016). ALPP is an alkaline phosphatase with ectopic expression observed in pancreatic cancer (Dua et al., 2013). Our data provide molecular evidence that TCDD activates several potential oncogenes and signaling pathways likely in an AHR-dependent manner. Because TCDD is a common and persistent environmental pollutant, it is possible that exposure to TCDD may contribute to

several types of cancers, as previously proposed by others (Poland et al., 1982). Indeed, pro-proliferative effects of TCDD have been shown in cell lines and rodent models of liver cancer (Poland et al., 1982).

To study the transcriptional outcomes of AHR inhibition in colon cancer cells, we performed RNA-seq in DLD1 cells treated with CH223191, a competitive inhibitor that prevents the binding of AHR to its ligands (Zhao et al., 2010). We have previously shown that colon cancer cells, which display elevated levels of AHR and Kyn, but not normal human colonic epithelial cells, are sensitive to CH223191 (Venkateswaran et al., 2019b).

Using the same approach as described for TCDD and Kyn, we compared the transcriptional signature regulated by CH223191 using DMSO as control. This approach identified 302 genes regulated by CH223191 (240 upregulated and 62 downregulated) (Fig. 1G, J). Unexpectedly, treatment with CH223191 caused broader effects on the transcriptional signature of DLD1 cells leading to both activated and repressed genes. CH223191 only inhibited the expression of 8 genes induced by TCDD including 3 genes that were also induced by Kyn (Fig. 1K). Gene ontology analyses revealed that CH223191 modulates the expression of genes that belong to multiple categories including tRNA synthesis and mTOR signaling (Fig. 1J). While CH223191 has been proposed as a potent inhibitor of TCDD-induced nuclear translocation of AHR (Zhao et al., 2010), it is possible that CH223191 has additional effects that could account for its ability to inhibit cell growth. Further studies on the off-target effects of CH223191 are necessary to define its specificity and clinical value. Furthermore, the development of new and improved inhibitors of AHR-ligand binding could lead to novel and more specific strategies to treat cancer.

Activation of AHR by TCDD and Kyn promotes the transcription of a common signature of genes

To characterize the canonical signature of ligand-activated AHR genes in colon cancer cells, we focused on the 6 genes co-regulated by Kyn and TCDD (Fig. 1M-N). This signature comprised an interesting and diverse group of genes: *CYP1A1*, *ALDH1A3*, *ABCG2*, *ADGFR1*, *SCIN* and *ITPR1* (Fig. 1O). *CYP1A1*, *ALDH1A3*, and *ABCG2* are involved in different aspects of drug metabolism or xenobiotic response. CYP1A1 metabolizes small molecules, leading to their clearance (e.g. etoposide and irinotecan) or to their conversion into carcinogens (e.g.

benzopyrenes) (Androutsopoulos et al., 2009; Badawi et al., 2001; McFadyen et al., 2004). ALDH1A3 is critical for the maintenance of cancer stem cells and is involved in the detoxification of aldehydes generated from alcohols and lipid peroxidation (Duan et al., 2016). ABCG2, previously named MDR1, is a well-characterized drug efflux pump that plays a vital role in resistance to chemotherapy (eg, irinotecan and methotrexate) (Robey et al., 2007). ABCG2 was previously shown to be regulated by AHR in esophageal squamous cell carcinoma (To et al., 2012) and upon its activation with pesticides in livestock (Kuhnert et al., 2020).

ADGRF1 is a G protein-coupled receptor involved in transmembrane signaling (Lee et al., 2016). ITPR1 is an ion channel involved in the release of calcium from the endoplasmic reticulum that has also been shown to protect cancer cells from NK cell-mediated death (Decuypere et al., 2015). Finally, the actin severing protein SCIN, also known as adseverin, plays a vital role in cytoskeletal organization and is important for cancer cell proliferation, migration, epithelial-to-mesenchymal transition, and CDC42-induced filopodia formation (Chen et al., 2014; Messai et al., 2014; Zunino et al., 2001).

To determine whether this gene signature was directly regulated by AHR, we searched for XRE elements (AHR-binding sites) in their regulatory regions. Bioinformatics analyses predicted that all 6 genes contained one or more XRE elements (Fig. S3A-F), further indicating that these could be direct transcriptional targets of AHR. The localization of these XRE elements in relationship to the transcription start site is listed in Fig. S3G). By examining a ChIP-seq data set deposited in the ENCODE database, we found that among the 6 genes, 2 (*CYP1A1* and *ITPR*) were strongly bound by AHR in HepG2 cells (Fig. S3A, F), while the other 4 displayed weaker interaction (Fig. S3B-E).

AHR ligands promote the expression of the 6-gene signature identified by RNA-seq

To validate the induction of these genes by AHR ligands, we performed RT-qPCR for *CYP1A1*, *ALDH1A3*, *ABCG2*, *ADGFR1*, *SCIN* and *ITPR1* in DLD1 cells incubated with Kyn, FICZ, TCDD, and quercetin (Fig. 2A) for 4 h and 8 h. All ligands were confirmed to promote the translocation of AHR into the nucleus of DLD1 cells (Fig. 2B). Kyn activated *CYP1A1*, *ALDH1A3*, *ABCG2*, and *ADGFR1* genes more efficiently at 4 h than 8 h. TCDD, on the other hand, had more dramatic effects at 8 h, potentially explaining the elevated number of target genes regulated by TCDD identified by RNA-seq at the 8-h time point. Incubation with FICZ

resulted in wider induction of all the target genes at both 4 h and 8 h (Fig. 2C-H). Quercetin activated *CYP1A1* and *ADGFR1* at both 4 h and 8 h, but none of the other target genes. Indeed, quercetin is the least potent ligand in driving nuclear translocation of AHR in DLD1 cells (Fig. 2B). *CYP1A1* was the most readily activated gene by all 4 ligands. FICZ was the strongest inducer of *CYP1A1* followed by Kyn, TCDD, and quercetin. Furthermore, to evaluate the expression of these 6 genes in response to AHR ligands in other cell lines, we performed RT-qPCR for the same genes in HCT116, HCT15, and HT29 cells incubated with DMSO or Kyn (20 μM) (Fig. 2I-N). These results demonstrated that these 6 genes are likely regulated in a cell type–specific manner with ALDH1A3 induced by Kyn in all tested lines and ABCG2 induced in none. Thus, our results identified a signature of genes regulated by ligands used to stimulate AHR translocation in colon cancer cells. These results suggest that different ligands of AHR have unique kinetics of AHR activation and that this should be considered when interpreting the potency of AHR ligands

Transcriptional activation of CYP1A1, ALDH1A3, ABCG2, ADGFR1, and SCIN by TCDD depends on AHR

To ascertain whether the induction of the genes identified by RNA-seq to be regulated by TCDD and Kyn was dependent on AHR, we generated stable DLD1 cells expressing shRNA targeting *AHR* or empty vector. We then confirmed that *AHR* mRNA (Fig. 3A) and protein (Fig. 3B) were downregulated in cells expressing shRNA targeting *AHR*. Importantly, incubation with ligands had no dramatic effects on the expression levels of AHR (Fig. 3A-B). These cell lines were then incubated with DMSO or TCDD, and the expression of the 6-gene signature was measured by RT-qPCR 8 h after ligand exposure (Fig. 3C-H). This experiment revealed that *CYP1A1*, as expected, was induced by TCDD, and this induction was dramatically reduced upon *AHR* knockdown, thus confirming that the induction of *CYP1A1* by TCDD requires AHR activity in colon cancer cells (Fig. 3C). Similarly, *ALDH1A3*, *ABCG2*, and *SCIN* exhibited increased expression upon incubation of DLD1 cells with TCDD, which was dependent on AHR expression (Fig. 3D-E, H). ITPR1, however, was the only gene of the colon cancer signature that did not display significant regulation by TCDD in the validation experiments, while it was regulated by FICZ (Fig. 3G and Fig. 2H). Due to their more robust regulation, we decided to focus on *CYP1A1*, *ALDH1A3*, *ABCG2*, and *SCIN* for further investigation.

To further validate the importance of AHR on the regulation of these genes, we used CRISPR to generate AHR knockout (KOs) lines using two independent AHR sgRNAs that were compared to cells expressing sgControl. Expression of CYP1A1, SCIN, and ABCG2 was attenuated in AHR KO cells, though ALDH1A3 levels are only slightly affected (Fig. 3I). These data confirm that AHR regulates CYP1A1, SCIN, and ABCG2 even in the absence of ligand stimulation. Additionally, we found that AHR KO cells displayed a significant lower proliferation than the control cells, thereby further confirming AHR's role in promoting cell proliferation in DLD1 cells (Fig. 3J).

Examining the TCGA database, we found no correlation between the expression of *CYP1A1*, *ALDH1A3*, *ABCG2*, *ADGFR1*, *SCIN* and *ITPR1* and patient survival for colon cancer (Fig. S4A). Moreover, the expression of these genes was not altered with tumor grade (Fig. S4B). We propose that the expression of *CYP1A1*, *ALDH1A3*, *ABCG2*, *ADGFR1*, and *SCIN* alone or in combination form a signature of genes expressed transiently in colon cancer cells upon exposure to AHR ligands.

SCIN is required for the growth of colon cancer cells

To determine the biological importance of the *CYP1A1*, *ALDH1A3*, *ABCG2*, *ADGFR1*, and *SCIN* for colon cancer cell growth, we used two independent siRNAs to knockdown the expression of each of these genes in DLD1 cells and measured cell viability. *ITPR1* was not evaluated for this experiment due to its minor regulation by TCDD and Kyn (Fig. 4F and 3G). The ability of each siRNA to reduce gene expression was validated using RT-qPCR 3 days after siRNA transfection in DLD1 cells (Fig. 5A-E). While siRNA for every target gene was effective at reducing gene expression (Fig. 5A-E), only *SCIN* knockdown caused a significant reduction in the growth of DLD1 cells with both siRNAs (Fig. 5J). Some genes such as *CYP1A1*, *ABCG2* and *ADGRF1* showed a marginal decrease in cell proliferation with only one of the siRNAs (Fig. 4F, H, and I).

To determine whether the sensitivity to *CYP1A1*, *ALDH1A3*, *ABCG2*, *ADGFR1*, and *SCIN* knockdown was altered in the presence of AHR ligands, we silenced each of the 5 genes with siRNA (Fig. 5A-E) and incubated cells in the presence of DMSO, TCDD, and Kyn (Fig. S5A-E). These data demonstrated that *SCIN* knockdown also reduced the viability of DLD1 cells grown in the presence of TCDD and Kyn (Fig. S5E), while *ADGFR1* only reduced the viability

in the presence of Kyn. This suggests that SCIN, and to a lower degree ADGFR1, are necessary for the growth of DLD1 cells.

Comparing the expression of *SCIN* by RT-qPCR in a panel of unstimulated colon cancer cell lines including DLD1, RKO, HCT15, HCT116, and HT29, we found that DLD1 expresses the highest levels of *SCIN* (Fig. 4K), in agreement with elevated levels of *AHR* in this cell line (Fig. 1A) followed by HT29 and HCT116. Therefore, to obtain a more diverse sample, we examined the importance of SCIN for the growth of HCT116 and HT29 cells. Given that HCT15 cells were isolated from the same patient as DLD1, we did not include HCT15 in further experiments. Interestingly, HT29 cells exhibited the most dramatic induction of SCIN upon ligand stimulation (Fig. 2M). Knocking down *SCIN* in HT29 and in HCT116 cells reduced cell viability (Fig. 4L), thus demonstrating that SCIN expression is broadly required for colon cancer growth. Nevertheless, stable shRNA-mediated knockdown of *SCIN* using two independent shRNAs did not significantly affect cell proliferation (Fig. S5F-G). It is likely that stable knockdowns allowed cellular adaptations to compensate for the reduction in SCIN levels. Our data is in agreement with the data from other studies showing that SCIN is necessary for the growth and aggressive behavior of colon cancer cells (Lin et al., 2019).

Expression of SCIN had modest but significant effects in the proliferation of colon cancer cells (Fig. 4M-N). While SCIN was first found to be highly expressed in normal cells of the kidney and intestines (Lueck et al., 1998), its function is now recognized as necessary for the proliferation of multiple cancer cell types (Chen et al., 2014; Lin et al., 2019; Zunino et al., 2001).

SCIN promotes nuclear translocation of β-catenin

To examine the cellular localization of V5-tagged SCIN that was ectopically expressed in DLD1 cells, we performed immunofluorescence using a V5 antibody and DAPI. We found that SCIN was localized in the cytoplasm, cellular periphery, and cell-cell junction domains, where actin also localizes (Fig. 5A). Hence, ectopically expressed SCIN displayed localization that is expected for the endogenous protein. Given the importance of SCIN in regulating the actin cytoskeleton, we asked whether SCIN expression affected actin dynamics. We first generated empty vector and SCIN-expressing lines to also express F-tractin tagged with GFP, an actin sensor. We then used time lapse microscopy to determine whether F-actin cytoskeleton was

affected by in SCIN-expressing cells. Examining filopodia, cell shape, and stress fibers, we found no measurable changes when comparing populations of cells expressing SCIN or empty vector (Fig. 5B and S6A). To quantify the ability of cell expressing SCIN or empty vector to attach to substrate, we measured the attachment of these cells 30 minutes after seeding (Fig S6B). Despite the addition of extracellular matrix to increase adhesion of these cells, there was no significant change in attachment in SCIN-expressing cells. There was a very modest trend to towards decreased adhesion upon SCIN-expression.

SCIN was shown to be involved in collagen degradation in MCF7 cells, which was proposed to affect matrix invasion and metastasis (Tanic et al., 2019). Previous studies found that elevated SCIN expression is associated with metastatic potential of colon cancer (Lin et al., 2019). To determine the importance of SCIN in the migration of DLD1 cells, we performed scratch assays comparing cells with SCIN overexpressed or knocked down. In both cases SCIN up or downregulation did not affect cell migration (Fig. S6 C-D).

Actin interacts intracellularly with cell-cell adhesion complex containing E-cadherin, β-catenin, and α-catenin and is part of a complex for cell adhesion that anchors the transmembrane protein E-cadherin. Upon activation of the WNT pathway, β-catenin translocates into the nucleus where it acts as a transcription factor in conjunction with members from the T-cell factor/Lymphoid enhancer factor (TCF/LEF) family to drive the expression of genes involved in cell proliferation and migration (MacDonald et al., 2009). In colon cancer cells (Fig. S5H), mutations in β-catenin's degradation machinery including AXIN and APC together with the kinases glycogen synthase kinase 3 (GSK3) and casein kinase 1 (CK1) can increases β-catenin levels and its nuclear activity. Other factors can also affect the signaling pool of β-catenin. For example, increased cell-cell adhesion, which occurs in cells grown at high density, recruits β-catenin to the membrane while single cell culture facilitates nuclear translocation of β-catenin (Conacci-Sorrell et al., 2003). This led us to hypothesize that SCIN, by altering the actin cytoskeleton, may affect the soluble pool of β-catenin.

By performing immunofluorescence using an antibody for β-catenin, we found that expression of SCIN led to an increase in the nuclear pool of β-catenin (Fig. 5B). Total levels of β-catenin were unaffected by SCIN up and downregulation (Fig. 5C). Nuclear and cytoplasmic fractionations of control or SCIN-expressing DLD1 cells demonstrated that SCIN promotes an increase in the nuclear pool of β-catenin (Fig. 5D). Additionally, nuclear and cytoplasmic

fractions of control versus SCIN knockdown cells demonstrated the reverse was also true with SCIN knockdown cells displaying slightly lower nuclear β-catenin levels than control cells.

We probed β-catenin levels in nuclear and cytoplasmic fractions from AHR knockout cells compared to control cells to determine whether a loss of AHR decreased nuclear β-catenin levels. Nuclear fractions of AHR knockout cells displayed a visible decrease in β-catenin (Fig. 5F), which collectively supports the model that AHR can affect the nuclear β-catenin pool through the regulation of SCIN.

To measure the transcriptional activity of β-catenin, we used a reporter gene that contains TCF/LEF binding sites fused with luciferase (TOPFlash). To account for specificity of the WNT pathway, the activity values obtained for TOPFlash activity were normalized by the values obtained by a mutant form of this motif that cannot bind TCF/LEF factors (FOPFlash). Experiments were performed as previously described (Hao et al., 2019) (Fig 5G, S6). Like the increase found in nuclear β-catenin in SCIN-expressing cells, we found that WNT signaling activity by the TOPFlash measurement was also elevated (Fig. 5H, S6F). Conversely, knocking down *SCIN* led to a modest reduction in TOPFlash activity (Fig. 5I, S6G), which is in line with the modest effects on the nuclear pool of β-catenin upon *SCIN* knockdown (Fig. 5E).

To explore whether the effects of SCIN upregulation could be attenuated by decreasing β-catenin/TCF transcription, we treated SCIN-expressing and control cells with ICG-001. ICG-001 decreased TOP/FOP values of both control and SCIN-expressing cells. Despite β-catenin inhibition, SCIN-expressing cells still showed an increase activity of β-catenin. These cells also showed reduced proliferation when treated with ICG-001 (Fig. 5M-N). Further analysis of downstream β-catenin target genes was addressed using Western blots (Fig. 5 K-L). These showed a a very slight increase of AXIN 2 in SCIN-expressing cells as compared to vector and a decrease in MYC and cyclin D1 (CD1) upon SCIN knockdown.

Examining normal and tumor samples of human colon cancer samples, we found that normal tissues did not express detectable levels of SCIN in the colon. However, matching samples of a subset of patients (38%, Fig. 5O) display elevated levels of SCIN in the tumors (example of a patient in Fig. 5P-Q). Other patients had low or undetectable levels (Fig. S6G). SCIN co-localized with nuclear β-catenin signal (Fig. 5Q). Using a collection of 37 human biopsy samples, we found that 38% of them had elevated levels of SCIN (Fig. 5O).

Our working model is that ligand-dependent activation of AHR leads to the expression of a signature of target genes that promote drug clearance (such as *CYP1A1*, *ABCG2* and *ALDH1A3*) and cell growth such as *SCIN*. SCIN, by altering the actin cytoskeleton, allows the nuclear translocation of β-catenin either by releasing it from junctions or by additional unknown mechanisms. Nuclear β-catenin activates the WNT pathway to drive cell growth (Fig. 6).

DISCUSSION

Our work demonstrates that AHR ligands can induce overlapping signatures of genes in the same cell line, though the group of AHR targets regulated is likely cell type specific. Both Kyn and TCDD promote the expression of genes involved in xenobiotic response and growth. It is possible that endogenously produced ligands such as Kyn are in part responsible for chemoresistance through the activation of AHR. This is supported by several studies which demonstrate a correlation between IDO1 expression and chemoresistance (Zhao et al., 2020) (Campia et al., 2015). As inducing the expression of genes such as *CYP1A1*, *ALDH1A3* and, *ABCG2*, have been shown to play an active role in eliminating the byproducts of the chemotherapeutic agents such as irinotecan, etoposide, and methotrexate (Zheng, 2017), this connection is further bolstered. Therefore, preventing the activation of AHR using pharmacological inhibitors in conjunction with chemotherapy may offer a means to help improve patient outcomes.

Of the six genes identified to be transcriptionally activated by AHR ligands in colon cancer cells, we have identified SCIN as an important contributor to cell growth and as a novel WNT pathway activator. Beyond its known actin severing properties, SCIN possesses the ability to selectively enrich the nuclear β-catenin pool and promote TCF-mediated transcription. We demonstrated that expression of SCIN leads to an increase in cancer cell growth and a correlative increase in nuclear β-catenin. These findings are in agreement with recent studies that demonstrated AHR's activation resulted in increased nuclear β-catenin in breast cancer stem cells, where AHR expression was elevated (Al-Dhfyan et al., 2017; Mohamed et al., 2019). It is possible that SCIN activity contributes to WNT pathway activation also in breast cancer. Interestingly, a recent study identified how APC mutation activating β-catenin could generate an oncogenic axis which in turn activates AHR in in colon cancer (Park et al., 2020). Therefore,

while multiple mechanisms inducing β-catenin accumulation may exist, AHR and β-catenin do appear to have prevalent crosstalk that is still being investigated.

High SCIN expression could represent a strategy for tumors to stimulate sufficient WNT pathway activity, which may explain why high SCIN expression correlates to metastasis in colon cancer (Lin et al., 2019). While there is much information on how transcriptional activity regulates cytoskeleton, there are limited examples of how morphological changes may translate into signaling and transcriptional events (Park et al., 2020). Our work proposes that alterations in SCIN levels and activity is a new example of how cytoskeletal changes regulate transcriptional activity of the WNT pathway.

MATERIAL AND METHODS

Cell culture

The colon cancer cell lines DLD1, HCT116, HCT15, RKO and HT29 were grown in DMEM (4500 mg/L glucose) with L-glutamine and sodium pyruvate and supplemented with 10% fetal bovine serum. All cells were purchased from ATCC and tested for contamination before experiments. For attachment assays, DLD1 cells expressing vector or SCIN were seeded in a 96-well plate (1 million cells/well), with or without coating of 1% collagen or 1% Matrigel. After 30 minutes of incubating at 37 C°, the cells were washed with PBS, and attached cells were fixed with methanol and stained with 0.1% crystal violet. The dye was stripped using 10% acetic acid and absorbance was measured using 595 nm. Cell motility was assessed using the scratch wound healing method. Cells were seeded at 90% confluency 24-well plates (Abcam). Using the area of the scratch as the cell motility parameter, we quantified the results by using the online software ImageJ.

For AHR CRISPR knockout cell lines, AHR sgRNA CRISPR/CAS9 All-in-One Lentivector or Scrambled sgRNA CRISPR/Cas9 All-in-One Lentivector was transfected together with lentiviral packaging plasmids pSPAX2 and pMD2g to HEK293FT cells. The conditional media of transfected cells (viruses) were filtered with 0.45 μM filter and used to infect DLD1 cells. Knockout cells were selected with 10 μg/mL puromycin, and single clones were picked to confirm the knockout. All sgRNA were obtained from Applied Biological Material.

RNA-seq analysis

DLD1 colon cancer cells incubated with DMSO, TCDD, or Kyn for 1 h were harvested and subjected to RNA-seq as previously described (Lafita-Navarro et al., 2018). The quality of sequencing reads were evaluated using NGS QC Toolkit (v2.3.3) (Patel and Jain, 2012) and high-quality reads were extracted. The human reference genome sequence and gene annotation data hg38 were downloaded from Illumina iGenomes. (https://support.illumina.com/sequencing/sequencing_software/igenome.html). The qualities of RNA-sequencing libraries were estimated by mapping the reads onto human transcript and ribosomal RNA sequences (Ensembl release 89) using Bowtie (v2.3.2) (Langmead and Salzberg, 2012). STAR (v2.5.2b) (Dobin et al., 2013) was used to align the reads onto the human and viral genomes. SAMtools (v1.9) (Li et al., 2009) was used to sort the alignments, and HTSeq Python package was used to count reads per gene (Anders et al., 2015). DESeq2 R Bioconductor package was used to normalize read counts and identify differentially expressed (DE) genes (Gentleman et al., 2004) (Anders and Huber, 2010). KEGG (Kanehisa et al., 2017) pathway data was downloaded using KEGG API (https://www.kegg.jp/kegg/rest/keggapi.html) and gene ontology (GO) data was downloaded from NCBI FTP (ftp://ftp.ncbi.nlm.nih.gov/gene/DATA/gene2go.gz). The enrichment of DE genes to pathways and GOs were calculated by Fisher's exact test in R statistical package.

Cell line production

Recombinant lentiviruses were produced by transfecting HEK293T Phoenix-amphotropic packaging cells with pMD2G (VSV-G protein), pPAX2 (lentivirus packaging vector), and lentiviral constructs using Lipofectamine 3000. Recombinant lentiviruses were harvested 48 h and 72 h after transfection, filtered, and used to infect the colon cancer cells, which were selected with puromycin. shRNA SCIN lentiviral bacterial stocks were purchased from Sigma (TRCN0000116622-TRCN0000116626). For infections, 50,000 DLD1, HCT116 and HT29 cells were seeded into 6-well plates with 1 mL media and 2 μL polybrene. Each well received either 1 mL of 293T-produced lentivirus (PLKO- empty vector, or shSCIN). Two days later, the medium was exchanged for fresh medium containing antibiotics needed for selection (10 mg/mL or 5 mg/mL puromycin or 5 mg/mL blasticidin). For ectopic expression of SCIN, vector was purchased from Genecopoeia (EX-Z6199-LX304). GFP-Ftractin (9-52 of the enzyme IPTKA30

fused to eGFP) was introduced in the cells using the pLVX lentiviral system (Clontech) and selected using antibiotic resistance to puromycin. For AHR CRISPR knockout cell lines, AHR sgRNA CRISPR/CAS9 All-in-One Lentivector or Scrambled sgRNA CRISPR/Cas9 All-in-One Lentivector was transfected together with lentiviral packaging plasmids pSPAX2 and pMD2g to HEK293FT cells. The conditional media of transfected cells (viruses) were filtered with 0.45 μM filter and used to infect DLD1 cells. Knockout cells were selected with 10 μg/mL puromycin, and single clones were picked to confirm the knockout. All sgRNA were obtained from Applied Biological Material.

Western blotting

Cells were lysed in RIPA buffer (25 mM Tris-HCl pH 7.4, 150 mM NaCl, 1% NP-40, 0.5% sodium deoxycholate, 0.1% SDS + protease and phosphatase inhibitors and MG132) for total protein extracts. Cytoplasmic extracts were isolated using buffer A (10 mM HEPES, 60 mM KCl, 1 mM EDTA, 0.075% [v/v] NP-40 with protease and phosphatase inhibitors and MG132). The remaining pellets are then washed twice with buffer A and resuspended in RIPA, sonicated and centrifuged at maximum speed for 15 min. Nuclear fractions were collected from the supernatants. All protein lysates were processed for Western blotting, and the samples were run on a gradient acrylamide gel (4-12%) and transferred to a nitrocellulose membrane. Membranes were blocked with 10% milk or 5% BSA in TBS-T for 1 h at room temperature or overnight and incubated overnight with primary antibodies dissolved in TBS-T 1% BSA. Membranes were washed the next day with TBS-T for 10 min 3 times before adding corresponding secondary antibodies dissolved in 5% milk or 1% BSA in TBS-T for 1 h at room temperature. Membranes were once again washed 3 times with TBS-T for 10 min and then visualized using the Bio Rad Chemidoc system. Antibodies were as follows: AHR polyclonal antibody (1:1000 Enzo Life Sciences 50-201-1848), Histone H3 antibody (1:2000 Cell Signaling, 4499S), GAPDH antibody (1:1000 Abcam, 9484), β-catenin antibody (1:2000 Cell Signaling, 2698S), Cyclin D1 antibody (1:1000 Cell Signaling, 2978S), Axin2 antibody (1:1000 abcam, ab109307), SCIN antibody (1:500 Santa Cruz, sc-376136), CYP1A1 antibody (1:1000 Sigma, SAB2108545), ABCG2 antibody (1:1000 Cell Signaling, 42078S), ALDH1A3 antibody (1:1000 Novus, NBP2-15339), Tubulin antibody (1:5000 Sigma T6199-200ml), and MYC antibody (1:1000 Abcam, 32072).

RT-qPCR

For RT-qPCR, RNA was extracted using the RNA extraction kit (Qiagen). Complementary DNA was generated by Superscript III (Invitrogen) and used with SYBR Green PCR master mix (Applied Biosystem) for RT-qTPCR analysis. The mRNA content was normalized to RPS18. All assays were performed using an Applied Biosystems Prism 7900HT sequence detection system and Bio-rad CFX. For each mRNA assessment, quantitative RT-PCR analyses were repeated at least twice with n=3. Primers used for qPCR: GAPDH F Human 5-TCGTGGAAGGACTCATGACCA, GAPDH R Human 5-AGGCAGGGATGATGTTCTGGA, ITPR1 F1 Human 5-GCGGAGGGATCGACAAATGG, ITPR1 R1 Human 5-TGGGACATAGCTTAAAGAGGCA, ITPR1 F2 Human 5-CCACAGACGCAGTGCTACTC, ITPR1 R2 Human 5-GTCCCCAGCAATTTCCTGTTT, SCIN F1 Human 5-ATGGCTTCGGGAAAGTTTATGT, SCIN R1 Human 5-CATCCACCATATTGTGCTGGG, ADGRF1 F1 Human 5-ACAGGGGAAACATCACAGCCA, ADGRF1 R1 Human 5-AAGGATGACACAGCTGCCTCA, CYP1A1 F1 Human 5-TCGGCCACGGAGTTTCTTC, CYP1A1 R1 Human 5-GGTCAGCATGTGCCCAATCA, ALDH1A3 F1 Human 5-TGAATGGCACGAATCCAAGAG, ALDH1A3 R1 Human 5-CACGTCGGGCTTATCTCCT, ABCG2 F1 Human 5-CAGGTGGAGGCAAATCTTCGT, and ABCG2 R1 Human 5-ACCCTGTTAATCCGTTCGTTTT.

Cell growth analyses

Cells were seeded at 10,000 cells/mL in 24-well plates, in triplicates, and 25,000 cells/mL in 6-well plates in triplicates. After 24 h cells were transfected with Lipofectamine RNAiMAX (Life technology 13778100), and 40 nM siRNA was used. After 96 h, the cells were fixed with methanol and stained with 0.1% crystal violet dissolved in 20% methanol. Cells were washed three times and de-stained with 10% acetic acid, the absorbance of this solution was measured at 595 nm to obtain relative proliferation. Alternatively, cells were seeded at 2000 cells/well in 96-well plates in octuplicates with 5 pmol siRNA. After 96 h, 10% WST-8 medium was added to the cells, which were then incubated for 1.5 h, and analyzed by measuring absorbance at 460 nm (Fig. 1B-D, 4N, 5M-N). For the ligand experiments cells were seeded and treated in the same manner, 24 h after transfection with siRNA the cells were exposed to Kyn (20 µM), TCDD (1 nM) and DMSO (control). siRNA used: SASI_Hs02_00325415 siSCIN A,

SASI_Hs02_00325416 siSCIN B, SASI_Hs02_00321614 siITPR1 A, SASI_Hs02_00321615 siITPR1 B, SASI_Hs01_00243010 siADGRF1 A, SASI_Hs01_00243011 siADGRF1 B, SASI_Hs01_00129096 siALDH1A3 A, SASI_Hs01_00129097 siALDH1A3 B, SASI_Hs01_00067924 siCYP1A1 A, SASI_Hs01_00067925 siCYP1A1 B, SASI_Hs01_00136087 siABCG2 A, SASI_Hs01_00136088 siABCG2 B, SASI_Hs02 00332182 siAHR, SIC001-10NMOL Mission siRNA Universal Negative Control #1, all from Sigma.

TOPFlash Luciferase Assays

For the LEF/TCF promoter activity assays, 1.5×10^5 empty vector (and pLKO) DLD1 cells and DLD1 cells with SCIN expression or knockdown seeded in triplicate in 12-well plates were transfected with the M50 Super 8x TOPFlash (Addgene # 12456) with seven TCF/LEF binding (Korinek et. al. 1997 SCIENCE[27]) or control M51 Super 8X FOPFlash plasmids (with seven copies of mutated TCF/LEF consensus sequence) (Korinek et al., 1997; Veeman et al., 2003). Cells were lysed with Glo Lysis Buffer (Promega) 48 h after transfection. Luciferase activity was measured with ONE-Glo™ Luciferase Assay System (Promega) and normalized with FOPFlash samples. All experiments were performed at least two times and each experiment contained three technical replicates. Statistical analyses were performed by t-test and statistical significance was established by a $P \leq 0.05$ for every experiment.

Immunohistochemistry, Immunofluorescence and Light Sheet Microscopy

Tissue sections (4 mm) were deparaffinized, dehydrated, and pretreated for 10 min in Dako buffer pH 6 (in a microwave or pressure cooker). Primary antibody diluted in RPMI 1640 + 10% bovine serum (9E10 at 1:175; 274 at 1:4) was added to the section and incubated overnight at 4°C. TBS/0.1% Tween 20 was used to wash the slides twice. Slides were developed with the EnVision System (Dako) and AEC for visualization according to the manufacturer's instructions. Immunofluorescence stainings were performed in glass cover glasses (0.16 to 0.19 mm). Cells were fixed with 4% paraformaldehyde, permeabilized with 0.5% Triton X-100, and blocked with 5% BSA for 1 h at room temperature. Samples were incubated with primary antibody for 1 h at room temperature or overnight at 4°C. Alexa secondary antibody (1:500) was used. DAPI (1 µg/mL), phalloidin (1:100) and V5 (1:250) were used to visualize the nucleus,

actin filaments and SCIN, respectively. For the Light Sheet Microscopy, imaging was performed with cells plated on 35-mm dish with cover glass bottom (P35G-1.5–14 C, Mattek). Imaging was done using oblique plane microscope (OPM) that uses a bespoke glass-tipped tertiary objective with optical shearing as described before (Chang et al., 2021; Sapoznik et al., 2020). Imaging was done in a chamber at 37ºC providing 5% CO_2 with exposure time of 20 min. The deconvolution was performed in 3D by using the blind deconvolution routine in MATLAB R2020a with a synthetic PSF and 10 iterations.

Chemicals and inhibitors

TCDD (Cambridge Isotope Laboratories Inc), Kyn (Sigma), FICZ (Sigma-Aldrich), CH-223191 (S7711, Selleck Chemicals) and quercetin (Cayman Chemical) were dissolved in DMSO. Equivalent volume of DMSO was used in control conditions.

AUTHOR CONTRIBUTIONS

N.V., L.P-C., RG, M.C.L.N., Y-H.H., EE, performed experiments. J.K. and L.X analyzed RNA-Seq. R.F., E.S., and B-J. C performed light sheet microscopy, N.V., RG, L.P-C., and M.C-S. designed the experiments and wrote the manuscript. The authors declare no potential conflicts of interest.

Acknowledgements

The work was financially supported by Cancer Prevention and Research Institute of Texas (CPRIT) (RP220046), American Cancer Society 724003, Welch Foundation I-2058-20210327, NCI R01CA245548, NIGMS GM145744-01 and the Circle of Friend's award to MCS and Rally Foundation, Children's Cancer Fund (Dallas, TX) and the Cancer Prevention and Research Institute of Texas (RP180319 and RP180805) to LX. MCS is the Virginia Murchison Linthicum Scholar in Medical Research.

References

Anders, S. and Huber, W. (2010). Differential expression analysis for sequence count data. *Genome Biol* **11**, R106.

Anders, S., Pyl, P. T. and Huber, W. (2015). HTSeq--a Python framework to work with high-throughput sequencing data. *Bioinformatics* **31**, 166-9.

Andersson, P., McGuire, J., Rubio, C., Gradin, K., Whitelaw, M. L., Pettersson, S., Hanberg, A. and Poellinger, L. (2002). A constitutively active dioxin/aryl hydrocarbon receptor induces stomach tumors. *Proc Natl Acad Sci U S A* **99**, 9990-5.

Androutsopoulos, V. P., Tsatsakis, A. M. and Spandidos, D. A. (2009). Cytochrome P450 CYP1A1: wider roles in cancer progression and prevention. *BMC Cancer* **9**, 187.

Badawi, A. F., Cavalieri, E. L. and Rogan, E. G. (2001). Role of human cytochrome P450 1A1, 1A2, 1B1, and 3A4 in the 2-, 4-, and 16alpha-hydroxylation of 17beta-estradiol. *Metabolism* **50**, 1001-3.

Chen, X. M., Guo, J. M., Chen, P., Mao, L. G., Feng, W. Y., Le, D. H. and Li, K. Q. (2014). Suppression of scinderin modulates epithelialmesenchymal transition markers in highly metastatic gastric cancer cell line SGC7901. *Mol Med Rep* **10**, 2327-33.

Clevers, H., Loh, K. M. and Nusse, R. (2014). Stem cell signaling. An integral program for tissue renewal and regeneration: Wnt signaling and stem cell control. *Science* **346**, 1248012.

Conacci-Sorrell, M., Simcha, I., Ben-Yedidia, T., Blechman, J., Savagner, P. and Ben-Ze'ev, A. (2003). Autoregulation of E-cadherin expression by cadherin-cadherin interactions: the roles of beta-catenin signaling, Slug, and MAPK. *J Cell Biol* **163**, 847-57.

Denison, M. S. and Nagy, S. R. (2003). Activation of the aryl hydrocarbon receptor by structurally diverse exogenous and endogenous chemicals. *Annu Rev Pharmacol Toxicol* **43**, 309-34.

Denison, M. S., Pandini, A., Nagy, S. R., Baldwin, E. P. and Bonati, L. (2002). Ligand binding and activation of the Ah receptor. *Chem Biol Interact* **141**, 3-24.

Dobin, A., Davis, C. A., Schlesinger, F., Drenkow, J., Zaleski, C., Jha, S., Batut, P., Chaisson, M. and Gingeras, T. R. (2013). STAR: ultrafast universal RNA-seq aligner. *Bioinformatics* **29**, 15-21.

Dua, P., Kang, H. S., Hong, S. M., Tsao, M. S., Kim, S. and Lee, D. K. (2013). Alkaline phosphatase ALPPL-2 is a novel pancreatic carcinoma-associated protein. *Cancer Res* **73**, 1934-45.

Duan, J. J., Cai, J., Guo, Y. F., Bian, X. W. and Yu, S. C. (2016). ALDH1A3, a metabolic target for cancer diagnosis and therapy. *Int J Cancer* **139**, 965-75.

Elsir, T., Smits, A., Lindstrom, M. S. and Nister, M. (2012). Transcription factor PROX1: its role in development and cancer. *Cancer Metastasis Rev* **31**, 793-805.

Feng, S., Cao, Z. and Wang, X. (2013). Role of aryl hydrocarbon receptor in cancer. *Biochim Biophys Acta* **1836**, 197-210.

Fukunaga, B. N., Probst, M. R., Reisz-Porszasz, S. and Hankinson, O. (1995). Identification of functional domains of the aryl hydrocarbon receptor. *J Biol Chem* **270**, 29270-8.

Gentleman, R. C., Carey, V. J., Bates, D. M., Bolstad, B., Dettling, M., Dudoit, S., Ellis, B., Gautier, L., Ge, Y., Gentry, J. et al. (2004). Bioconductor: open software development for computational biology and bioinformatics. *Genome Biol* **5**, R80.

Han, H., Davidson, L. A., Hensel, M., Yoon, G., Landrock, K., Allred, C., Jayaraman, A., Ivanov, I., Safe, S. H. and Chapkin, R. S. (2021). Loss of Aryl Hydrocarbon Receptor Promotes Colon Tumorigenesis in Apc(S580/+); Kras(G12D/+) Mice. *Mol Cancer Res* **19**, 771-783.

Hao, Y. H., Lafita-Navarro, M. C., Zacharias, L., Borenstein-Auerbach, N., Kim, M., Barnes, S., Kim, J., Shay, J., DeBerardinis, R. J. and Conacci-Sorrell, M. (2019). Induction of LEF1 by MYC activates the WNT pathway and maintains cell proliferation. *Cell Commun Signal* **17**, 129.

Ikuta, T., Kobayashi, Y., Kitazawa, M., Shiizaki, K., Itano, N., Noda, T., Pettersson, S., Poellinger, L., Fujii-Kuriyama, Y., Taniguchi, S. et al. (2013). ASC-associated inflammation promotes cecal tumorigenesis in aryl hydrocarbon receptor-deficient mice. *Carcinogenesis* **34**, 1620-7.

Ikuta, T., Tachibana, T., Watanabe, J., Yoshida, M., Yoneda, Y. and Kawajiri, K. (2000). Nucleocytoplasmic shuttling of the aryl hydrocarbon receptor. *J Biochem* **127**, 503-9.

Janiszewska, M., Primi, M. C. and Izard, T. (2020). Cell adhesion in cancer: Beyond the migration of single cells. *J Biol Chem* **295**, 2495-2505.

Kanehisa, M., Furumichi, M., Tanabe, M., Sato, Y. and Morishima, K. (2017). KEGG: new perspectives on genomes, pathways, diseases and drugs. *Nucleic Acids Res* **45**, D353-D361.

Kawajiri, K., Kobayashi, Y., Ohtake, F., Ikuta, T., Matsushima, Y., Mimura, J., Pettersson, S., Pollenz, R. S., Sakaki, T., Hirokawa, T. et al. (2009). Aryl hydrocarbon receptor suppresses intestinal carcinogenesis in ApcMin/+ mice with natural ligands. *Proc Natl Acad Sci U S A* **106**, 13481-6.

Koliopanos, A., Kleeff, J., Xiao, Y., Safe, S., Zimmermann, A., Buchler, M. W. and Friess, H. (2002). Increased arylhydrocarbon receptor expression offers a potential therapeutic target for pancreatic cancer. *Oncogene* **21**, 6059-70.

Kubli, S. P., Bassi, C., Roux, C., Wakeham, A., Gobl, C., Zhou, W., Jafari, S. M., Snow, B., Jones, L., Palomero, L. et al. (2019). AhR controls redox homeostasis and shapes the tumor microenvironment in BRCA1-associated breast cancer. *Proc Natl Acad Sci U S A* **116**, 3604-3613.

Kuhnert, L., Giantin, M., Dacasto, M., Halwachs, S. and Honscha, W. (2020). AhR-activating pesticides increase the bovine ABCG2 efflux activity in MDCKII-bABCG2 cells. *PLoS One* **15**, e0237163.

Lafita-Navarro, M. C., Kim, M., Borenstein-Auerbach, N., Venkateswaran, N., Hao, Y. H., Ray, R., Brabletz, T., Scaglioni, P. P., Shay, J. W. and Conacci-Sorrell, M. (2018). The aryl hydrocarbon receptor regulates nucleolar activity and protein synthesis in MYC-expressing cells. *Genes Dev* **32**, 1303-1308.

Lafita-Navarro, M. C., Perez-Castro, L., Zacharias, L. G., Barnes, S., DeBerardinis, R. J. and Conacci-Sorrell, M. (2020a). The transcription factors aryl hydrocarbon receptor and MYC cooperate in the regulation of cellular metabolism. *J Biol Chem*.

Lafita-Navarro, M. C., Venkateswaran, N., Kilgore, J. A., Kanji, S., Han, J., Barnes, S., Williams, N. S., Buszczak, M., Burma, S. and Conacci-Sorrell, M. (2020b). Inhibition of the de novo pyrimidine biosynthesis pathway limits ribosomal RNA transcription causing nucleolar stress in glioblastoma cells. *PLoS Genet* **16**, e1009117.

Langmead, B. and Salzberg, S. L. (2012). Fast gapped-read alignment with Bowtie 2. *Nat Methods* **9**, 357-9.

Lee, J. W., Huang, B. X., Kwon, H., Rashid, M. A., Kharebava, G., Desai, A., Patnaik, S., Marugan, J. and Kim, H. Y. (2016). Orphan GPR110 (ADGRF1) targeted by N-docosahexaenoylethanolamine in development of neurons and cognitive function. *Nat Commun* **7**, 13123.

Li, H., Handsaker, B., Wysoker, A., Fennell, T., Ruan, J., Homer, N., Marth, G., Abecasis, G., Durbin, R. and Genome Project Data Processing, S. (2009). The Sequence Alignment/Map format and SAMtools. *Bioinformatics* **25**, 2078-9.

Lin, Q., Li, J., Zhu, D., Niu, Z., Pan, X., Xu, P., Ji, M., Wei, Y. and Xu, J. (2019). Aberrant Scinderin Expression Correlates With Liver Metastasis and Poor Prognosis in Colorectal Cancer. *Front Pharmacol* **10**, 1183.

Lueck, A., Brown, D. and Kwiatkowski, D. J. (1998). The actin-binding proteins adseverin and gelsolin are both highly expressed but differentially localized in kidney and intestine. *J Cell Sci* **111 (Pt 24)**, 3633-43.

MacDonald, B. T., Tamai, K. and He, X. (2009). Wnt/beta-catenin signaling: components, mechanisms, and diseases. *Dev Cell* **17**, 9-26.

Matthews, J., Wihlen, B., Thomsen, J. and Gustafsson, J. A. (2005). Aryl hydrocarbon receptor-mediated transcription: ligand-dependent recruitment of estrogen receptor alpha to 2,3,7,8-tetrachlorodibenzo-p-dioxin-responsive promoters. *Mol Cell Biol* **25**, 5317-28.

McFadyen, M. C., Melvin, W. T. and Murray, G. I. (2004). Cytochrome P450 enzymes: novel options for cancer therapeutics. *Mol Cancer Ther* **3**, 363-71.

Messai, Y., Noman, M. Z., Hasmim, M., Janji, B., Tittarelli, A., Boutet, M., Baud, V., Viry, E., Billot, K., Nanbakhsh, A. et al. (2014). ITPR1 protects renal cancer cells against natural killer cells by inducing autophagy. *Cancer Res* **74**, 6820-32.

Miyazaki, T., Chung, S., Sakai, H., Ohata, H., Obata, Y., Shiokawa, D., Mizoguchi, Y., Kubo, T., Ichikawa, H., Taniguchi, H. et al. (2022). Stemness and immune evasion conferred by the TDO2-AHR pathway are associated with liver metastasis of colon cancer. *Cancer Sci* **113**, 170-181.

Murray, I. A., Patterson, A. D. and Perdew, G. H. (2014). Aryl hydrocarbon receptor ligands in cancer: friend and foe. *Nat Rev Cancer* **14**, 801-14.

Narasimhan, S., Stanford Zulick, E., Novikov, O., Parks, A. J., Schlezinger, J. J., Wang, Z., Laroche, F., Feng, H., Mulas, F., Monti, S. et al. (2018). Towards Resolving the Pro- and Anti-Tumor Effects of the Aryl Hydrocarbon Receptor. *Int J Mol Sci* **19**.

Opitz, C. A., Litzenburger, U. M., Sahm, F., Ott, M., Tritschler, I., Trump, S., Schumacher, T., Jestaedt, L., Schrenk, D., Weller, M. et al. (2011). An endogenous tumour-promoting ligand of the human aryl hydrocarbon receptor. *Nature* **478**, 197-203.

Park, J. S., Burckhardt, C. J., Lazcano, R., Solis, L. M., Isogai, T., Li, L., Chen, C. S., Gao, B., Minna, J. D., Bachoo, R. et al. (2020). Mechanical regulation of glycolysis via cytoskeleton architecture. *Nature* **578**, 621-626.

Patel, R. K. and Jain, M. (2012). NGS QC Toolkit: a toolkit for quality control of next generation sequencing data. *PLoS One* **7**, e30619.

Petrova, T. V., Nykanen, A., Norrmen, C., Ivanov, K. I., Andersson, L. C., Haglund, C., Puolakkainen, P., Wempe, F., von Melchner, H., Gradwohl, G. et al. (2008). Transcription factor PROX1 induces colon cancer progression by promoting the transition from benign to highly dysplastic phenotype. *Cancer Cell* **13**, 407-19.

Poland, A., Palen, D. and Glover, E. (1982). Tumour promotion by TCDD in skin of HRS/J hairless mice. *Nature* **300**, 271-3.

Robey, R. W., Polgar, O., Deeken, J., To, K. W. and Bates, S. E. (2007). ABCG2: determining its relevance in clinical drug resistance. *Cancer Metastasis Rev* **26**, 39-57.

Rothhammer, V. and Quintana, F. J. (2019). The aryl hydrocarbon receptor: an environmental sensor integrating immune responses in health and disease. *Nat Rev Immunol* **19**, 184-197.

Tanic, J., Wang, Y., Lee, W., Coelho, N. M., Glogauer, M. and McCulloch, C. A. (2019). Adseverin modulates morphology and invasive function of MCF7 cells. *Biochim Biophys Acta Mol Basis Dis* **1865**, 2716-2725.

Tassi, E., Henke, R. T., Bowden, E. T., Swift, M. R., Kodack, D. P., Kuo, A. H., Maitra, A. and Wellstein, A. (2006). Expression of a fibroblast growth factor-binding protein during the development of adenocarcinoma of the pancreas and colon. *Cancer Res* **66**, 1191-8.

To, K. K., Yu, L., Liu, S., Fu, J. and Cho, C. H. (2012). Constitutive AhR activation leads to concomitant ABCG2-mediated multidrug resistance in cisplatin-resistant esophageal carcinoma cells. *Mol Carcinog* **51**, 449-64.

Tsay, J. J., Tchou-Wong, K. M., Greenberg, A. K., Pass, H. and Rom, W. N. (2013). Aryl hydrocarbon receptor and lung cancer. *Anticancer Res* **33**, 1247-56.

Tursynbay, Y., Zhang, J., Li, Z., Tokay, T., Zhumadilov, Z., Wu, D. and Xie, Y. (2016). Pim-1 kinase as cancer drug target: An update. *Biomed Rep* **4**, 140-146.

Van der Heiden, E., Bechoux, N., Muller, M., Sergent, T., Schneider, Y. J., Larondelle, Y., Maghuin-Rogister, G. and Scippo, M. L. (2009). Food flavonoid aryl hydrocarbon receptor-mediated agonistic/antagonistic/synergic activities in human and rat reporter gene assays. *Anal Chim Acta* **637**, 337-45.

Venkateswaran, N. and Conacci-Sorrell, M. (2020). Kynurenine: an oncometabolite in colon cancer. *Cell Stress* **4**, 24-26.

Venkateswaran, N., Lafita-Navarro, M. C., Hao, Y. H., Kilgore, J. A., Perez-Castro, L., Braverman, J., Borenstein-Auerbach, N., Kim, M., Lesner, N. P., Mishra, P. et al. (2019a). MYC promotes tryptophan uptake and metabolism by the kynurenine pathway in colon cancer. *Genes Dev*.

Venkateswaran, N., Lafita-Navarro, M. C., Hao, Y. H., Kilgore, J. A., Perez-Castro, L., Braverman, J., Borenstein-Auerbach, N., Kim, M., Lesner, N. P., Mishra, P. et al. (2019b). MYC promotes tryptophan uptake and metabolism by the kynurenine pathway in colon cancer. *Genes Dev* **33**, 1236-1251.

Xie, G., Peng, Z. and Raufman, J. P. (2012). Src-mediated aryl hydrocarbon and epidermal growth factor receptor cross talk stimulates colon cancer cell proliferation. *Am J Physiol Gastrointest Liver Physiol* **302**, G1006-15.

Yao, E. F. and Denison, M. S. (1992). DNA sequence determinants for binding of transformed Ah receptor to a dioxin-responsive enhancer. *Biochemistry* **31**, 5060-7.

Zhang, X., Liu, X., Zhou, W., Du, Q., Yang, M., Ding, Y. and Hu, R. (2021). Blockade of IDO-Kynurenine-AhR Axis Ameliorated Colitis-Associated Colon Cancer via Inhibiting Immune Tolerance. *Cell Mol Gastroenterol Hepatol* **12**, 1179-1199.

Zhao, B., Degroot, D. E., Hayashi, A., He, G. and Denison, M. S. (2010). CH223191 is a ligand-selective antagonist of the Ah (Dioxin) receptor. *Toxicol Sci* **117**, 393-403.

Zheng, H. C. (2017). The molecular mechanisms of chemoresistance in cancers. *Oncotarget* **8**, 59950-59964.

Zunino, R., Li, Q., Rose, S. D., Romero-Benitez, M. M., Lejen, T., Brandan, N. C. and Trifaro, J. M. (2001). Expression of scinderin in megakaryoblastic leukemia cells induces differentiation, maturation, and apoptosis with release of plateletlike particles and inhibits proliferation and tumorigenesis. *Blood* **98**, 2210-9.

Figures

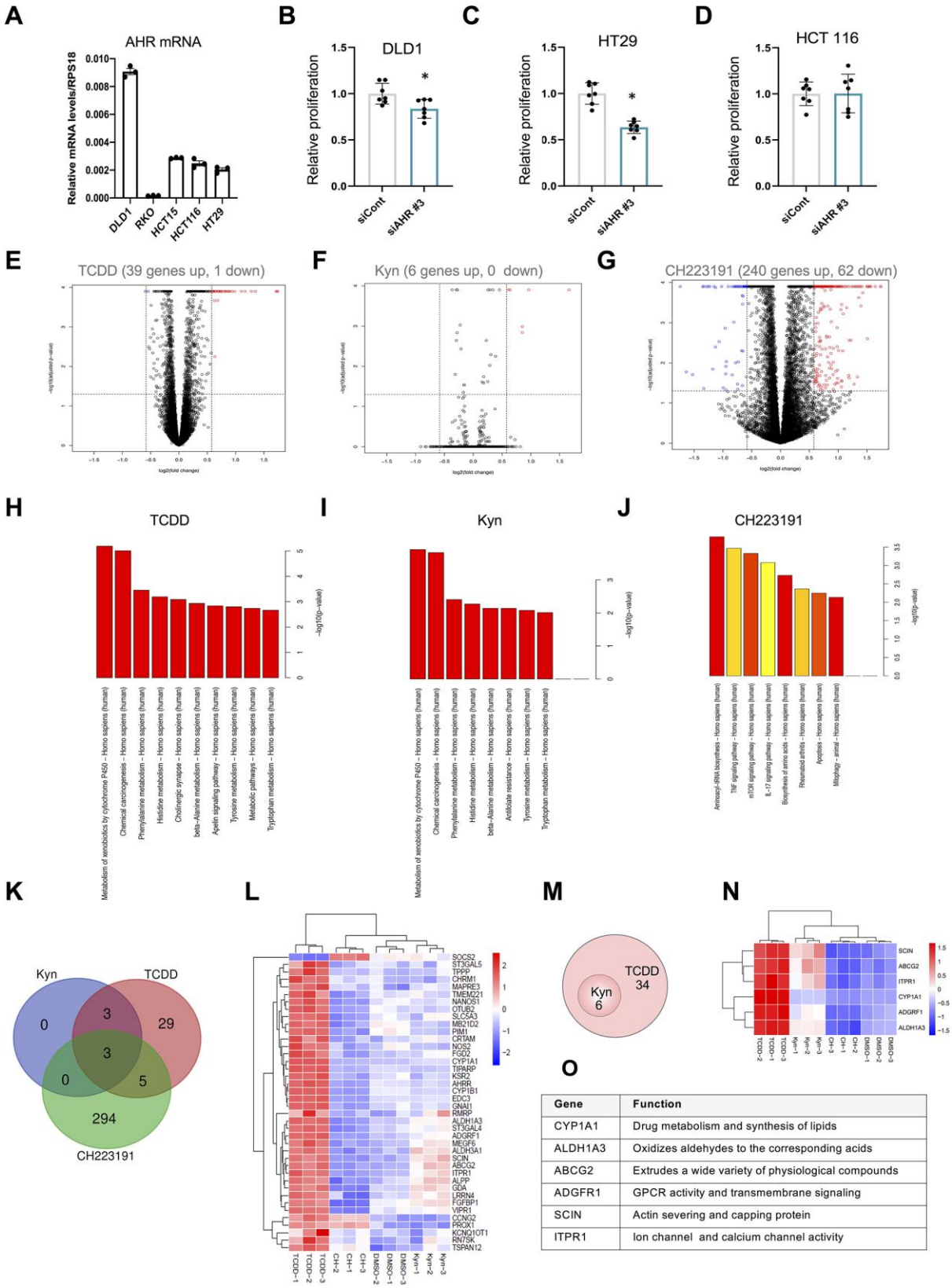

O

Gene	Function
CYP1A1	Drug metabolism and synthesis of lipids
ALDH1A3	Oxidizes aldehydes to the corresponding acids
ABCG2	Extrudes a wide variety of physiological compounds
ADGFR1	GPCR activity and transmembrane signaling
SCIN	Actin severing and capping protein
ITPR1	Ion channel and calcium channel activity

Fig. 1. RNA-seq identifies transcriptional signatures regulated by TCDD, Kyn, and the AHR inhibitor CH223191.

(A) RT-qPCR for AHR normalized to housekeeping gene RPS18 in a panel of colon cancer cell lines. (B) Relative proliferation at 460 nm absorbance of DLD1 cells after transfection with siRNA to knockdown AHR (C) Relative proliferation at 460 nm absorbance of HT29 cells after transfection with siRNA to knockdown AHR. (D) Relative proliferation at 460 nm absorbance of HCT116 cells after transfection with siRNA to knockdown AHR. B-D Experiments repeated twice. (E) Volcano plot showing the differentially expressed genes upon incubation with TCDD (1 nM). (F) Volcano plot showing the differentially expressed genes upon incubation with Kyn (10 µM), (G) Volcano plot showing the differentially expressed genes upon incubation with CH223191 (10 µM). (H) Gene ontology analysis showing the major pathways that are regulated upon incubation with TCDD. (I) Gene ontology analysis showing the major pathways that are regulated upon incubation with Kyn. (J) Gene ontology analysis showing the major pathways that are regulated upon incubation with CH223191. (K) Venn diagram showing the overlap of TCDD, Kyn and CH223191 regulated genes. (L) Heatmap of genes regulated by Kyn, TCDD and CH223191 after 8 h of treatment. For all analyses Log2FC $\leq$0.585 and adjusted p value $\leq$0.05 were applied. (M) Venn diagram showing the overlap of TCDD and Kyn regulated genes. (N) Heatmap of genes regulated by Kyn and TCDD after 8 h of incubation. (O) Molecular functions of the genes differentially expressed.

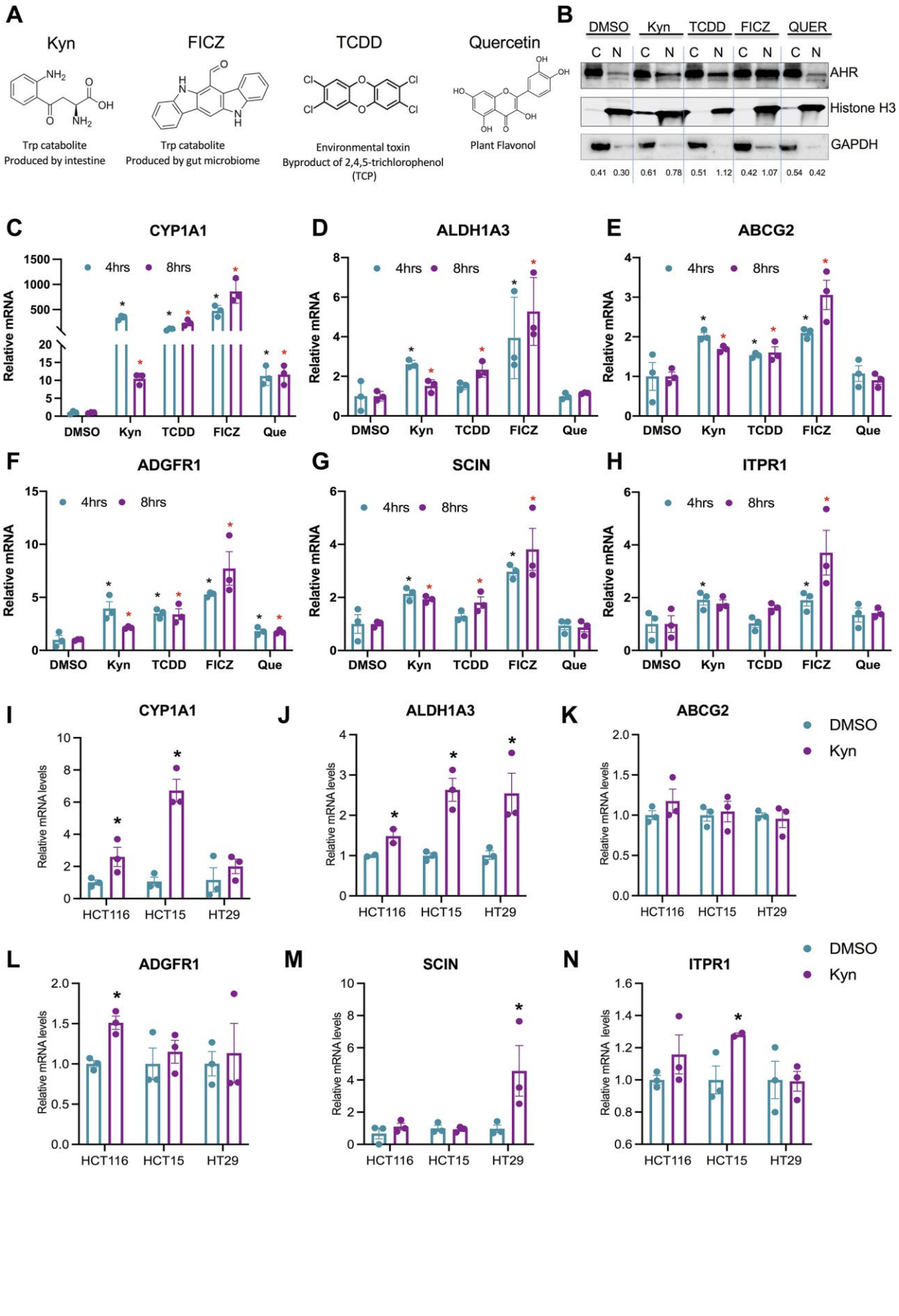

Fig. 2. Activation of AHR by TCDD and Kyn promotes the transcription of a common signature of genes.

(A) Schematic molecular structures of different ligands of AHR (Kyn, TCDD, FICZ and quercetin). (B) Western blot analysis showing the translocation of AHR upon treatment with DMSO, 1nM TCDD, 20 µM Kyn, 1 µM FICZ and 10 µM quercetin for 30 min in DLD1 cells. (C-H) qPCR validation of genes regulated by Kyn. DLD1 cells were treated with DMSO, 1 nM TCDD, 20 µM Kyn, 1 µM FICZ and 10 µM quercetin for 4 h and 8 h. Expression of the specified genes was normalized to RPS18. * P≤0.05 comparison between DMSO and each ligand at 4 h. * P≤0.05 comparison between DMSO and each ligand at 8 h. (I-N) RT-q-PCR for the expression of the indicated genes in colon cancer cell lines. HCT116, HCT15, and HT29 cells were incubated with DMSO or 20 mM Kyn for 8 h. Expression of the specified genes was normalized to RPS18. * p≤0.05 comparison between DMSO and Kyn for each cell line.

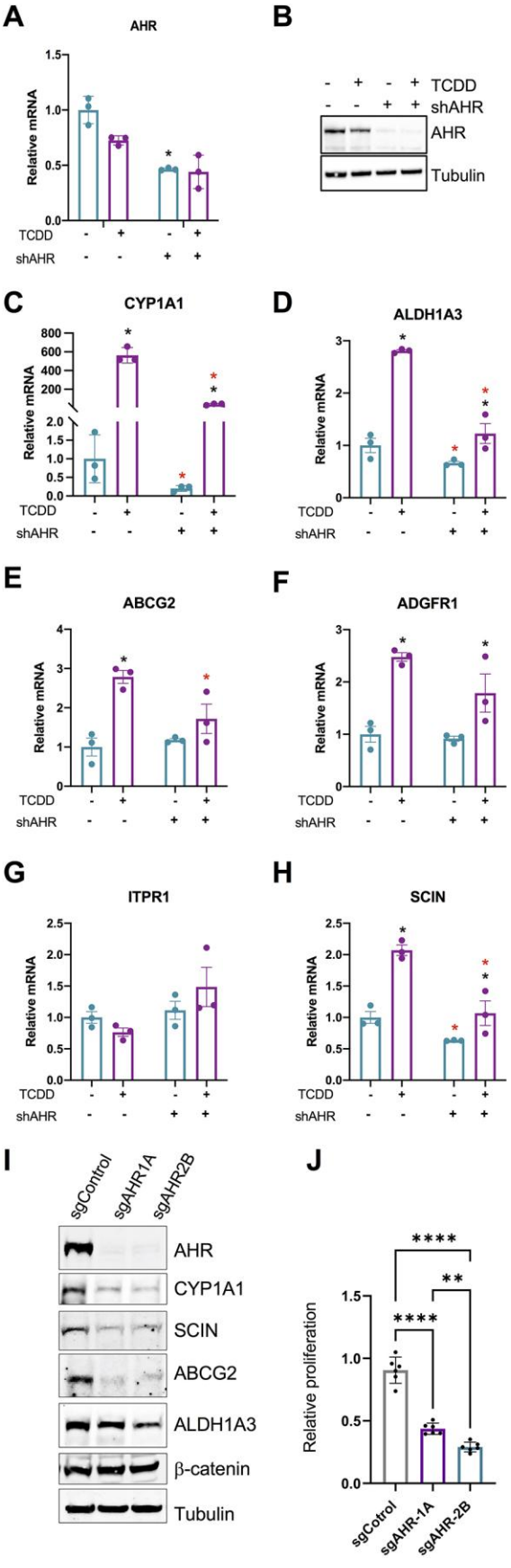

Fig. 3. Modulation of AHR activity by shAHR, TCDD, and Kyn regulate the transcription of a common signature of genes in colon cancer cells.

(A) RT-qPCR for *AHR* in DLD1 cells stably expressing empty vector or shRNA for AHR in the presence or absence of TCDD. (B) Western blot for AHR in DLD1 cells stably expressing empty vector or shRNA for AHR in the presence or absence of TCDD. (C-H) qPCR of genes regulated by AHR. DLD1 cells transduced with empty vector or shRNA targeting AHR incubated with DMSO or 1nM TCDD for 24 h. Expression of the specified genes was normalized to RPS18. Fold change obtained by normalizing to PLKO cells treated with DMSO. * $p \leq 0.05$ comparison between DMSO and TCDD. * $p \leq 0.05$ comparison between PLKO and shAHR. (I) Western blot for AHR, CYP1A1, SCIN, ABCG2. ALDH1A3, β-catenin, and tubulin in AHR CRISPR KO DLD1 cells. (J) Relative proliferation of DLD1 control and AHR CRISPR KO cells with crystal violet staining 4 days after seeding.

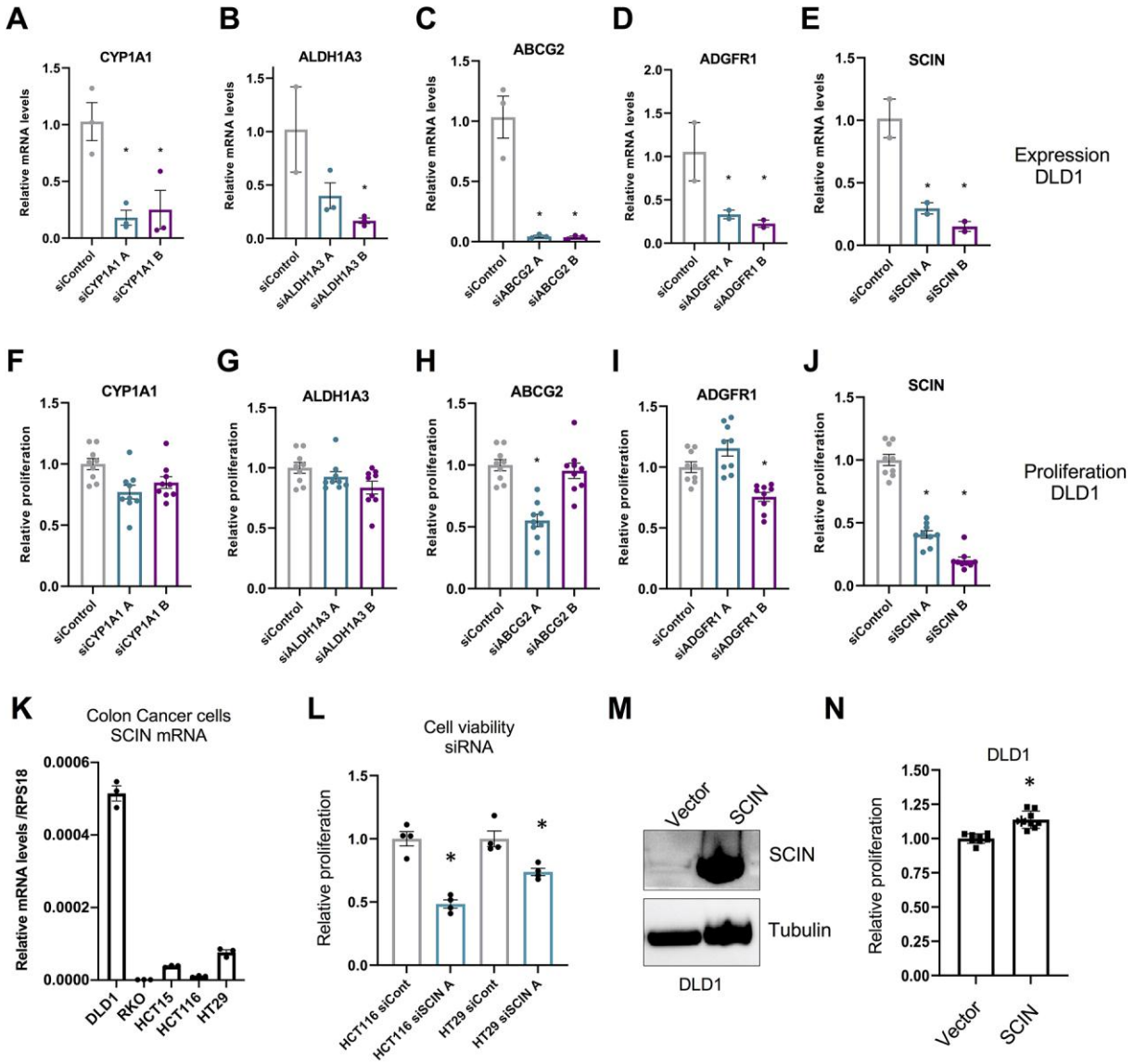

Fig. 4. SCIN is necessary for colon cancer cell viability.

(A-E) RT-qPCR of DLD1 cells transfected with siControl or siRNA targeting each of the indicated genes. Cells were harvested 3 days after siRNA transfection. Experiments repeated 3 times. (F-J) Relative proliferation of DLD1 cells quantified by crystal violet staining 6 days after transfection with control siRNA or siRNA targeting the indicated genes. Experiments were repeated 3 times. (K) RT-qPCR for *SCIN* in colon cancer cell lines. (L) Relative proliferation of

HCT116 and HT29 5 days after transfection with Control or siRNA targeting *SCIN*. Experiments were repeated twice. (M) Western blot of DLD1 cells stably expressing SCIN expression compared with empty vector (Vector). (N) Relative proliferation of DLD1 cells stably expressing SCIN compared with empty vector. * $p \leq 0.05$ comparison between siControl and gene targeting siRNAs

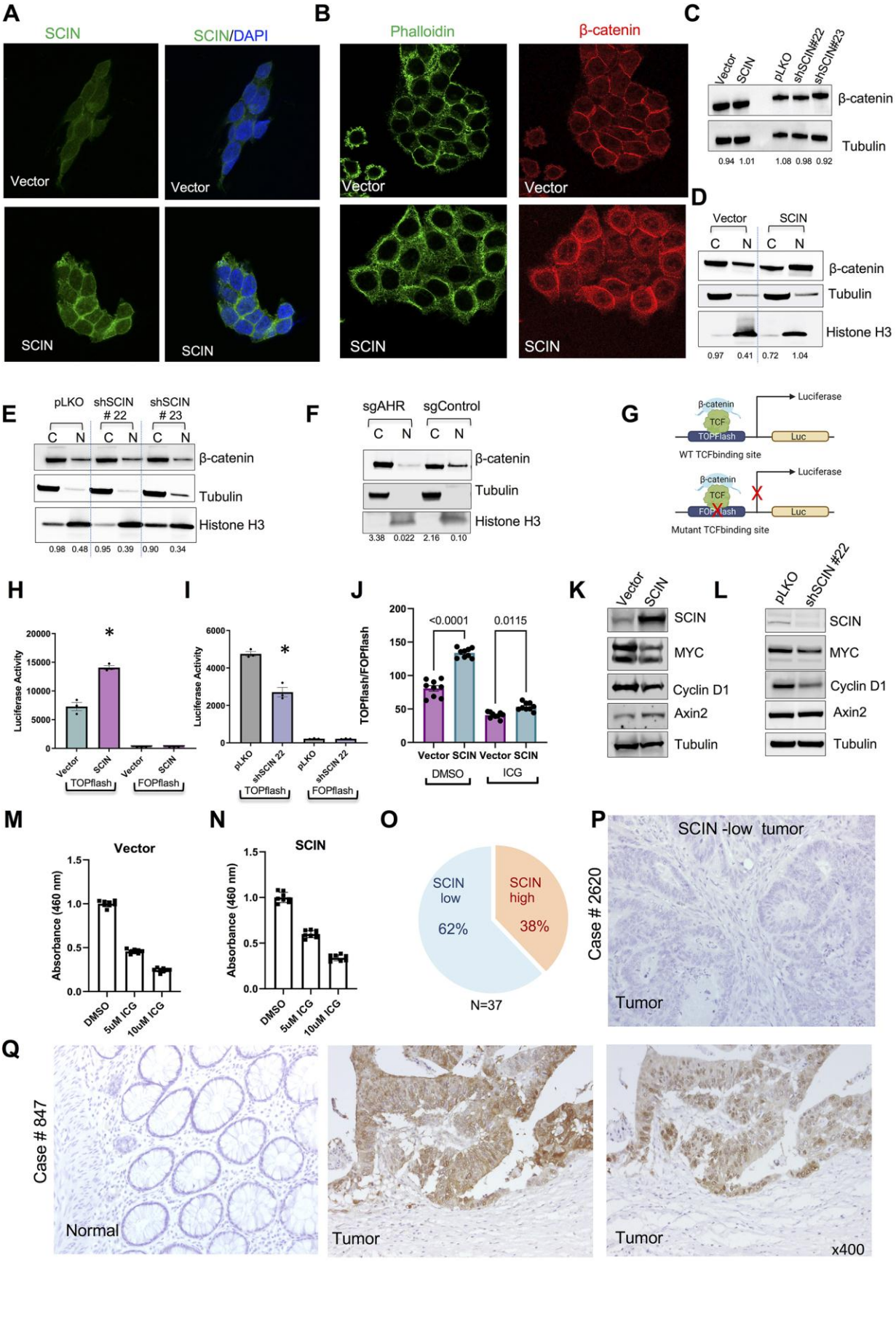

Fig. 5. SCIN expression promotes nuclear translocation of β-catenin.

(A) Immunofluorescence for SCIN (V5 tag) and nucleus (DAPI) (B) Immunofluorescence for actin and β-catenin of DLD1 cells expressing empty vector or SCIN. (C) Western blot for β-catenin and tubulin in lysates of DLD1 cells stably expressing vector (empty), SCIN, pLKO (Vector for shRNA), shSCIN#22, and shSCIN#23; showing that total β-catenin levels are not affected by SCIN expression. (D) Western blot of nuclear (N) and cytoplasmic (C) fractions of DLD1 cells stably expressing vector, or SCIN immunoblotted for β-catenin, tubulin, and histone H3. (E) Western blot of nuclear (N) and cytoplasmic (C) fractions of DLD1 cells stably expressing pLKO (vector for shRNA), and SCIN shRNAs: shSCIN#22 and shSCIN#23 immunoblotted for β-catenin, tubulin, and histone H3. (F) Western blot of nuclear (N) and cytoplasmic (C) fractions of DLD1 cells control and CRIPR AHR KO immunoblotted for β-catenin, tubulin, and histone H3. (G) Schematic representation of the β-catenin responsive report TOPFlash and its negative control FOPFlash. (H) DLD1 cells stably expressing vector or SCIN were transfected with TOPFlash or FOPFlash and luciferase reporter activity was measured 48 h later. Experiments were repeated 3 times. (I) DLD1 cells stably expressing empty vector (pLKO) and shRNA for SCIN were transfected with a TOPFlash or FOPFlash and processed as in (H). Experiments were repeated 3 times. (J) DLD1 cells stably expressing vector or SCIN were transfected with TOPFlash or FOPFlash and treated with 10 μM ICG-001, and luciferase reporter activity was measured 48 h later. Results were normalized by FOPflash. (K) Western Blot of Vector and SCIN DLD1 cells immunoblotting for SCIN, MYC, Cyclin D1, Axin 2, and Tubulin. (L) Western Blot of Vector (pLKO) and shSCIN #22 DLD1 cells immunoblotting for SCIN, MYC, Cyclin D1, Axin 2, and Tubulin. (M) Growth curve of Vector DLD1 cells after treatments with DMSO, 5 μM ICG-001, and 10 μM ICG-001. (N) Growth curve of SCIN DLD1

cells after treatments with DMSO, 5 μM ICG-001, and 10 μM ICG-001. (O) Quantification of SCIN expression in colon cancer patients comparing normal and tumor samples. (P) Example of tumor sample displaying low levels of SCIN expression measured IHC for SCIN. (Q) Representative immunohistochemistry for SCIN and β-catenin in biopsies from a patient with colon cancer containing normal and tumor tissues of the same patient.

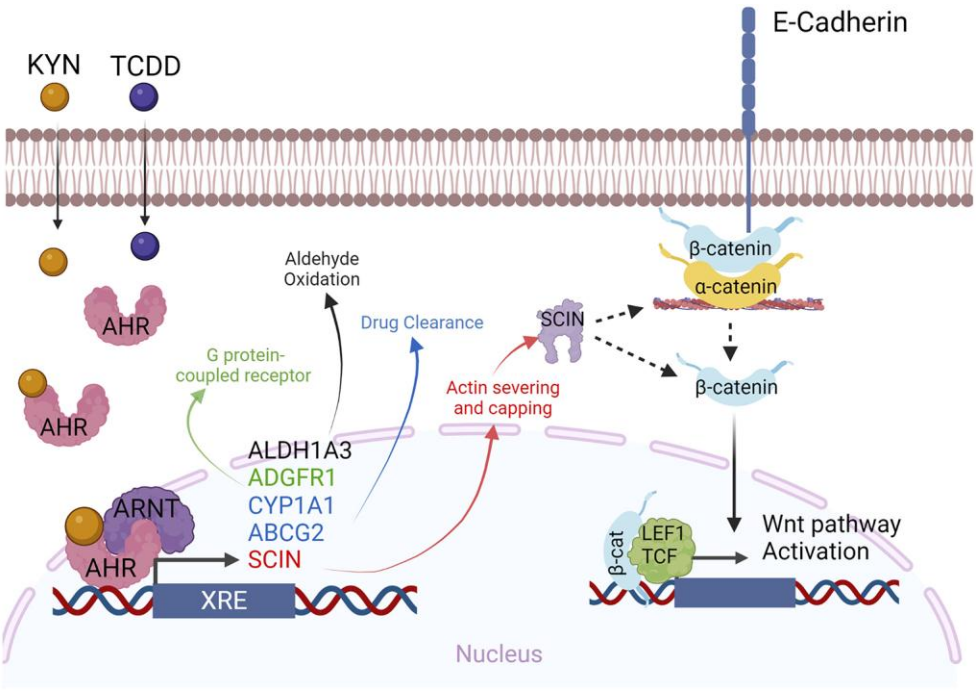

Fig. 6. Working models for the activation of AHR target genes in the presence of Kyn and TCDD. After ligand activation, AHR translocates into the nucleus where it dimerizes with ARNT. Activation of AHR regulates ALDH1A3, ADGFR1, CYP1A1, ABCG2, and SCIN. SCIN interacts with the actin cytoskeleton possibly releasing β-catenin from junctions. Free β-catenin translocates into the nucleus and regulates genes in the WNT pathway.

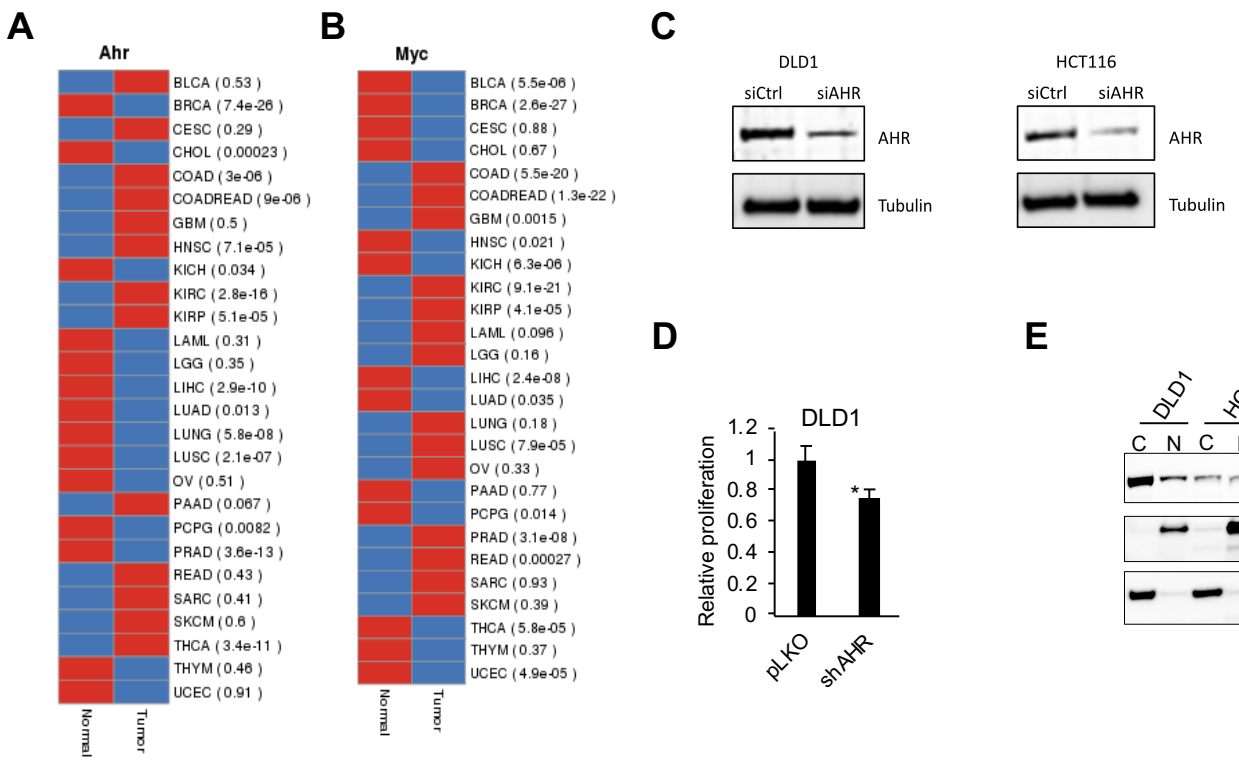

Fig. S1. (A) Heatmap showing AHR levels in Normal vs Tumor samples (TCGA database). (B) Heatmap showing MYC levels in Normal vs Tumor samples (TCGA database). (C) Western blot of DLD1 and HCT116 cells after shRNA transfection for AHR, immunoblotting for AHR and Tubulin. (D) Relative proliferation of DLD1 cells after shRNA transfection for AHR. (E) Western blot analysis of nuclear and cytoplasmic fractions of colon cancer cells for AHR. Expression levels of MYC and Tubulin were used as markers for nuclear and cytoplasmic fractions, respectively.

A

GENE	FUNCTION	
TPPP	Microtubule binding binding	Cytoskeleton
SCIN	Actin severing and capping	
GDA	Hydrolytic deamination of guanine	
MAPRE3	Microtubule elongation	
ANKRD13C	Molecular chaperone for G protein-coupled receptors	G-Protein signaling
CHRM1	Adenyl cyclase binding and ion channel modulator	
FGD2	Guanine nucleotide exchange factor	
ADGRF1	G protein-coupled receptor/transmembrane signaling	
VIPR1	G protein-coupled receptor/vasoactive intestinal polypeptide receptor	
ITPR1	Ion channel activity and calcium channel	
GNAI1	GTP binding and obsolete signal transducer	
SOCS2	Regulators of cytokine receptor signaling via the JAK/STAT pathway	Cellular signaling
DDIT4	Inhibitor of mTORC1	
CCNG2	Negative regulation of cell cycle progression	
KSR2	Negative regulator of RAS signaling	
TSPAN12	WNT-independent activation of beta-catenin	
SLC5A3	Transport glucose, hexose, bile salts	transporter
ABCG2	Extrudes of physiological compounds, dietary toxins and xenobiotics	
NANOS1	Translational repressor	RNA related genes
RMRP	Mitochondrial RNA processing endoribonuclease	
RN7SK	RNA Component Of 7SK Nuclear Ribonucleoprotein	
EDC3	Promotes efficient removal of the m7G cap from mRNAs	
NOS2	Nitric oxide synthase producing nitric oxide free radical	
ST3GAL4	Glycosyltransferase in protein glycosylation	
ST3GAL5	Catalyzes the formation of GM3 using lactosylceramide as the substrate	
FGFBP1	Fibroblast growth factor carrier protein	Potential oncogenes
KCNQ1OT1	Regulates transcription of multiple target genes through epigenetic modifications	
PROX1	Transcription factor	
PIM1	Ser/Thr protein kinase that plays a role in cell signaling	
ALPP	Metalloenzyme that catalyzes the hydrolysis of phosphoric acid monoesters	
AHRR	Repression of AHR-dependent gene expression	Canonical AHR targets
TIPARP	Inhibits transcription activator activity of AHR	
ALDH1A3	Aldehyde dehydrogenase enzyme	
ALDH3A1	Aldehyde dehydrogenases oxidize various aldehydes to the corresponding acids	
CYP1A1	Catalyzes reactions involved in drug metabolism and synthesis of lipids	
CYP1B1	Catalyzes many reactions involved in drug metabolism and synthesis of lipids	
CRTAM	Antigen presentation and innate immunity	
MEGF6	Calcium ion binding	
LRRN4	Hippocampus-dependent long-lasting memory	
OTUB2	Deubiquitylating enzyme	
MB21D2		
TMEM221		

B

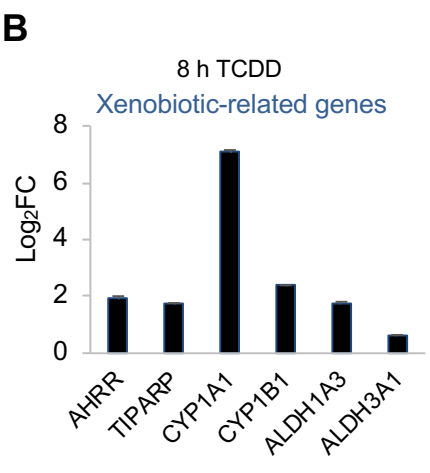

C

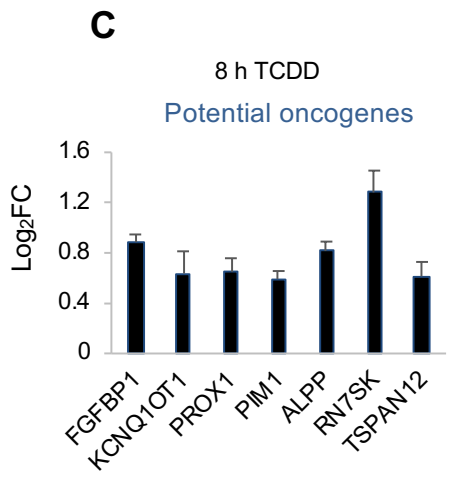

Fig. S2. (A) Table showing the functions of genes regulated by TCDD. (B) Expression of genes involved in xenobiotic response identified by RNA-seq upon incubation 1 nM TCDD for 8 h. (C) Expression of potential oncogenes genes identified by RNA-seq upon incubation 1 nM TCDD for 8 h Fold change of activated oncogenes upon treatment with 1 nM TCDD after 8 h.

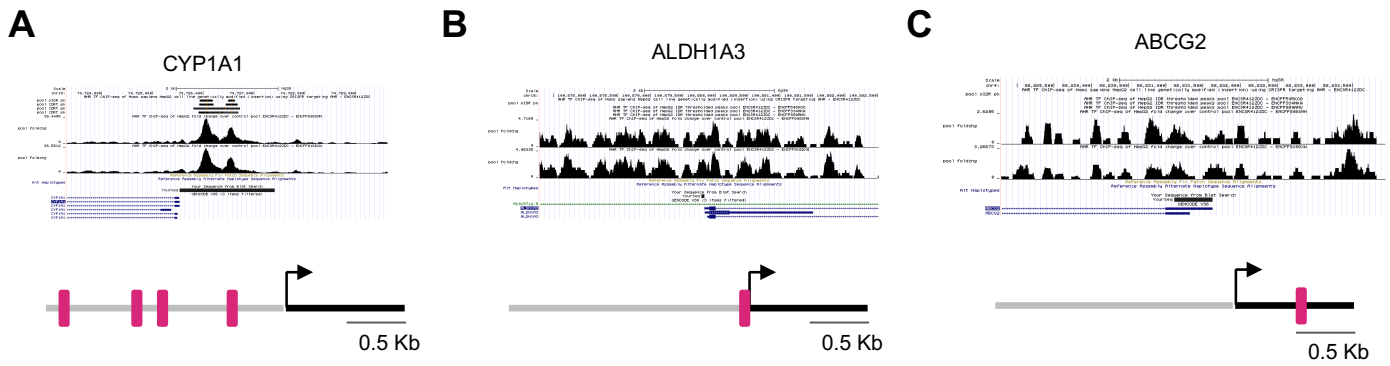

G

Gene	Position upstream TSS	Position downstream TSS
SCIN	151	55, 343
ITPR1	933, 547	240, 458, 861
CYP1A1	1869, 1252, 1051, 49	
ALDH1A3	43	
ADGRF1	25	
ABCG2		512

Fig. S3. (A-F) Promoters of all 6 genes with the localization of xenobiotic responsive elements (XRE) and ENCODE data from ChIP-seq done in HepG2. p≤0.05 comparison between DMSO and each ligand at 8 h. For all RNA-seq analyses Log2FC ≤0.585 and adjusted p ≤0.05 were applied. (G) Table showing the positions of the XRE motif in the 6 target genes.

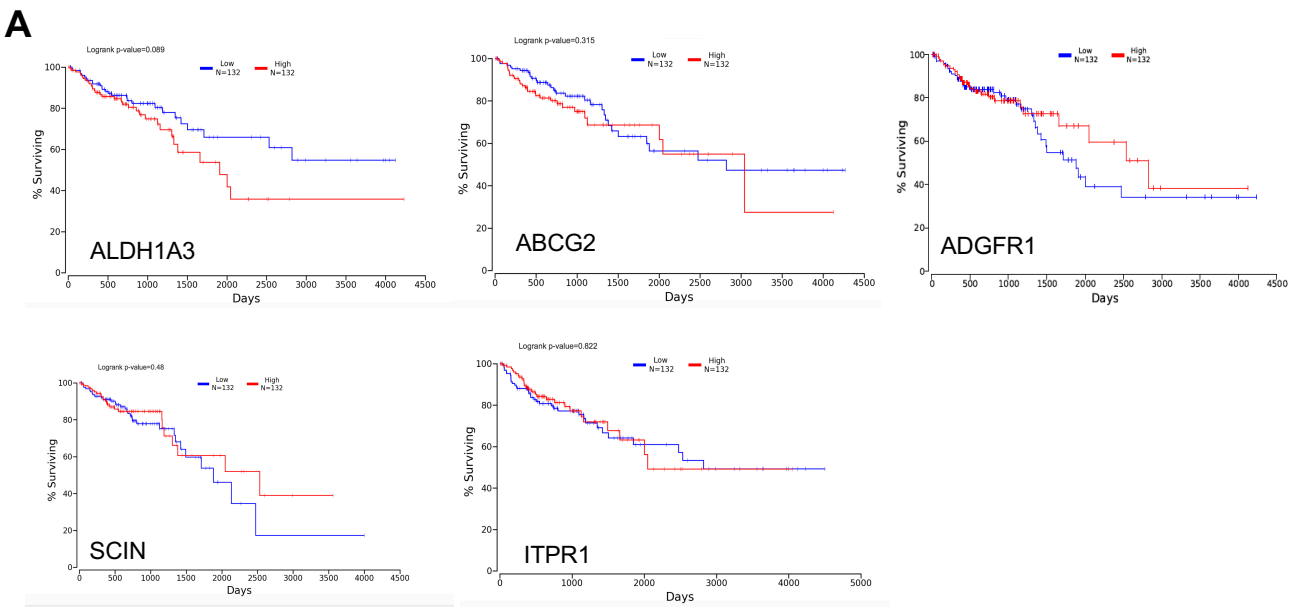

Fig. S4. (A) Kaplan-Meier curves correlating the expression of *ABCG2, ALDH1A3*, *ADGFR1*, *SCIN,* and *ITPR1* with colon cancer patient outcome using TCGA dataset. High=top 30%, Low=bottom 30%. Curves were generated using http://www.oncolnc.org. Correlation between *CYP1A1* and colon cancer was not available. (B) Expression of *CYP1A1, ABCG2, ALDH1A3*, *ADGFR1, SCIN*, and *ITPR1* in colon cancer samples deposited in the TCGA and grouped per tumor stage.

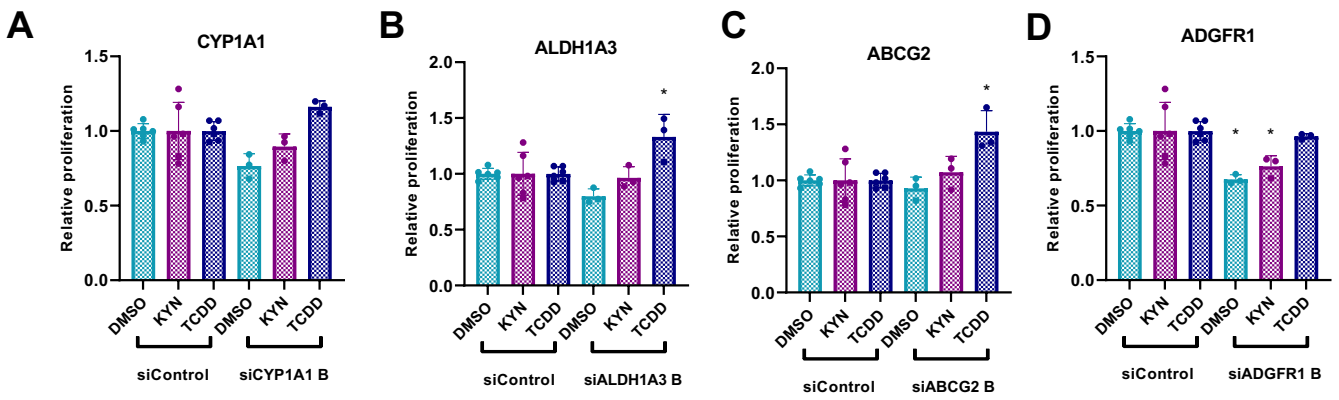

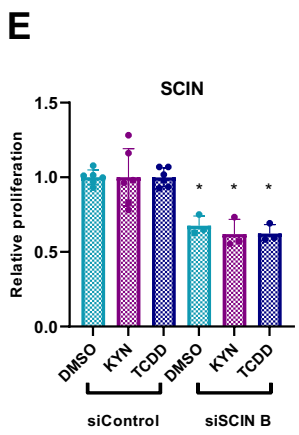

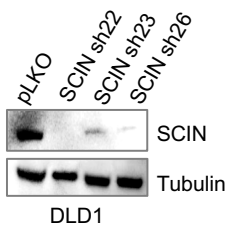

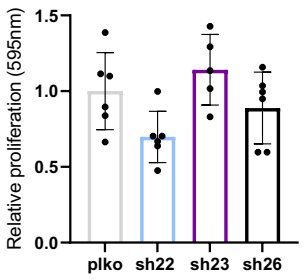

H

Cell line	Cell type	Gender	Age	APC	β-catenin	Ras	p53	AHR mRNA	b-cat protein	TopFLASH
DLD1	epithelial	male	adult	truncated	WT	G13D	Mutated	++++	+++	++
HT29	epithelial	female	44	truncated	WT	WT	Mutated	++	+++	++
HCT116	epithelial	male	adult	WT	mutated	G13D	WT	++	++	+++
HCT15	epithelial	male	adult	truncated	WT	G13D	Mutated	++	ND	ND
RKO	epithelial	female	82	WT	WT	WT	WT	+	+	+

Fig. S5. (A-E) Relative proliferation of DLD1 cells after silencing of each gene using siRNA in the presence of DMSO, TCDD (1 nM) or Kyn (20 μM). (F) Western blot of DLD1 stable lines after transfection with shRNA for SCIN. (G) Relative proliferation of DLD1 cells pLKO, shSCIN22, and shSCIN23. (H) Table providing information of different colon cancer cell lines.

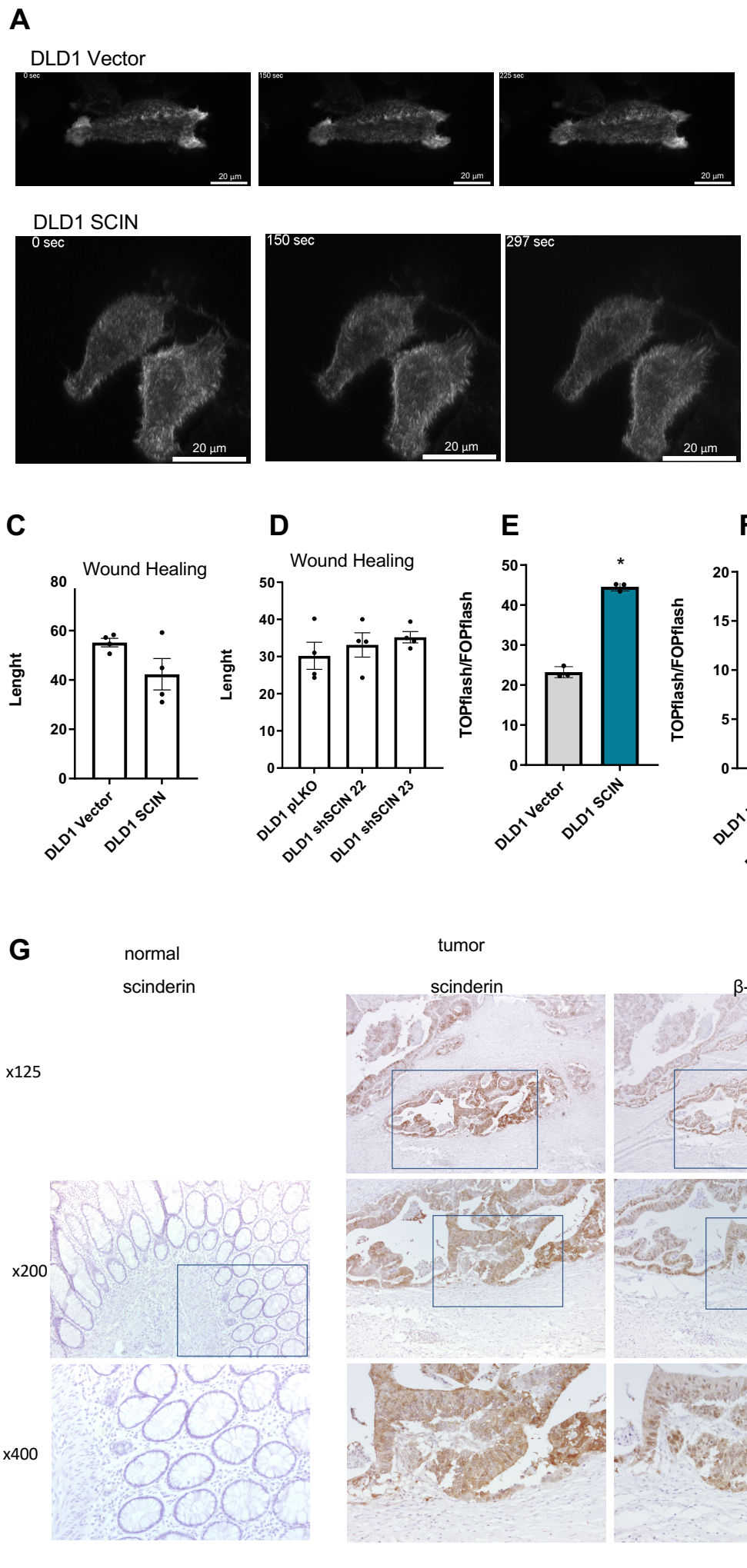

Fig. S6. (A) Snapshots of DLD1 Vector and SCIN cells using light sheet microscopy for f-actin. (B) Relative attachment of DLD1 expressing vector and SCIN cells 30 minutes after seeding and stained by crystal violet. (C-D) Wound healing assay of DLD1 vector, SCIN, pLKO, shSCIn #22, and shSCIN#23 cells. (E-F) DLD1 cells stably expressing vector, SCIN, pLKO or shSCIN #22 were transfected with TOPFlash or FOPFlash, and luciferase reporter activity was measured 48 h later. (G) IHC staining of SCIN and β-catenin in normal tissue vs tumor tissue from patients with colon cancer.

Table S1. TCDD_RNA-seq. For all analyses Log2FC ≤0.585 and adjusted p value ≤0.05 were applied.

Click here to download Table S1

Table S2. Kyn_RNA-seq. For all analyses Log2FC ≤0.585 and adjusted p value ≤0.05 were applied.

Click here to download Table S2

Table S3. CH_RNA-seq. For all analyses Log2FC ≤0.585 and adjusted p value ≤0.05 were applied.

Click here to download Table S3